KINETIC STUDIES OF ION-MOLECULE REACTION IN GAS PHASE: MODELS AND EXPERIMENTS

EMIE-UP
Multiscale Dynamics in Molecular Systems
August 2019

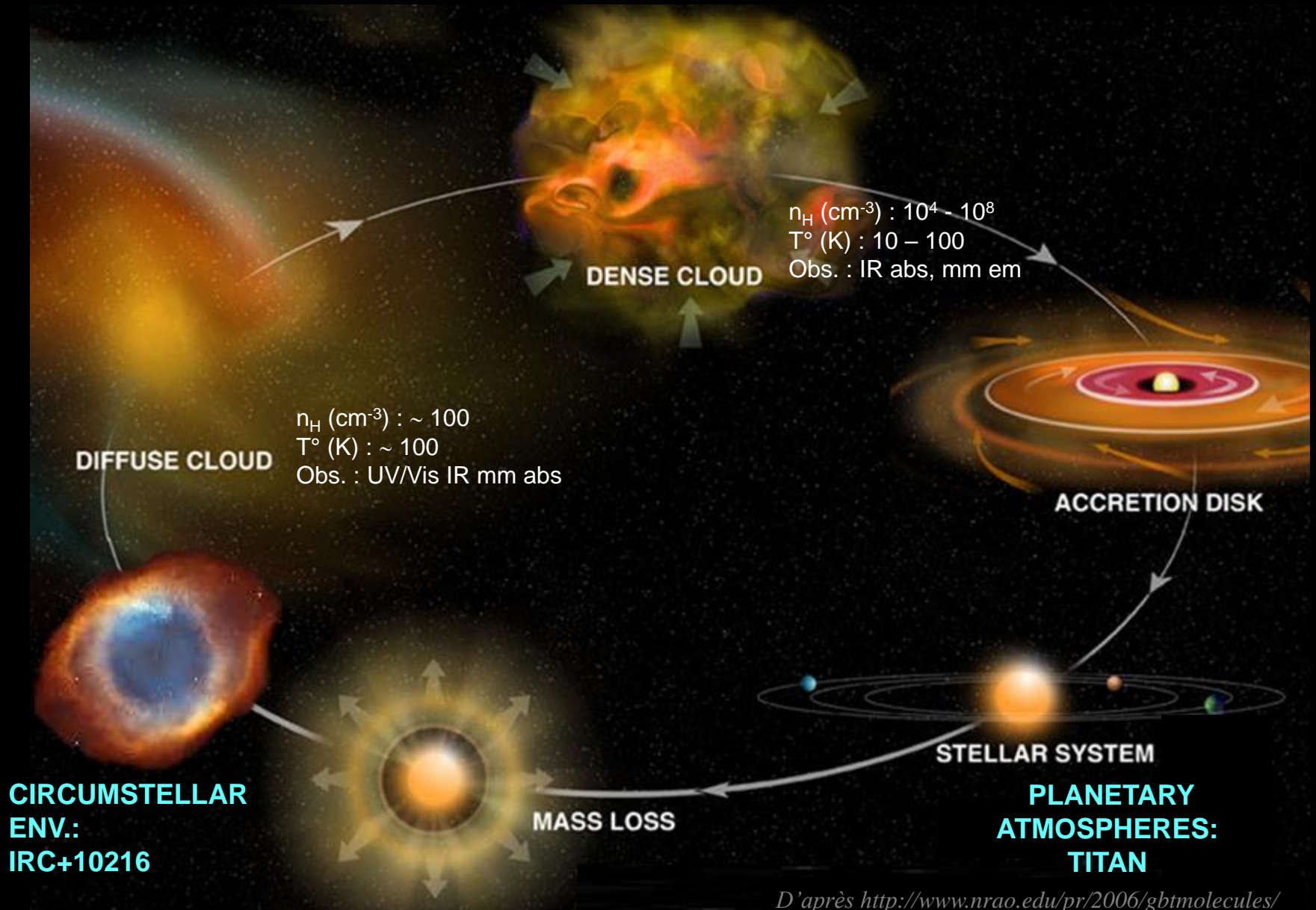## SOPHIE CARLES

Laboratory Astrophysics group

Physics Institut of Rennes IPR

University of Rennes 1

1

Cold Chemistry in Gas Phase

n_H (cm^{-3}) : 10^4 - 10^8
T° (K) : 10 – 100
Obs. : IR abs, mm em

DENSE CLOUD

ACCRETION DISK

n_H (cm^{-3}) : ~ 100
T° (K) : ~ 100
Obs. : UV/Vis IR mm abs

DIFFUSE CLOUD

STELLAR SYSTEM

CIRCUMSTELLAR ENV.: IRC+10216

MASS LOSS

PLANETARY ATMOSPHERES: TITAN

D'après http://www.nrao.edu/pr/2006/gbtmolecules/

P. Hily Blant

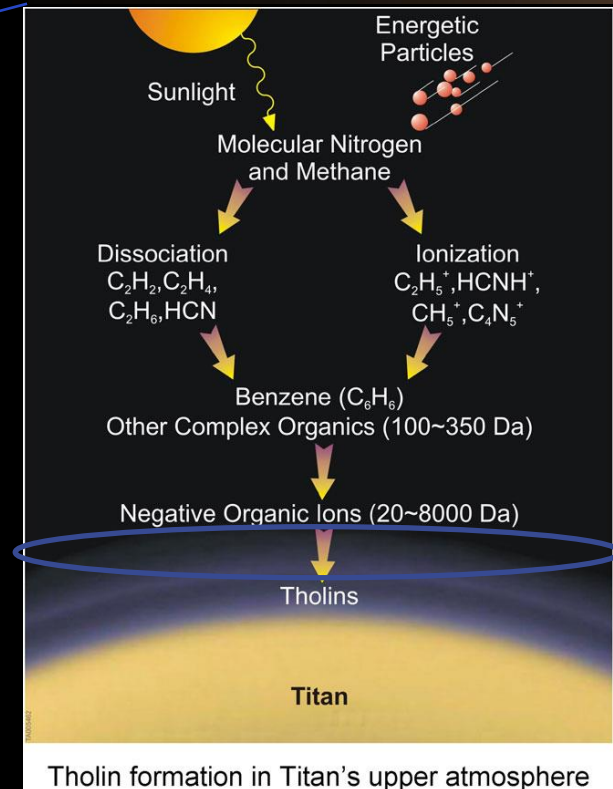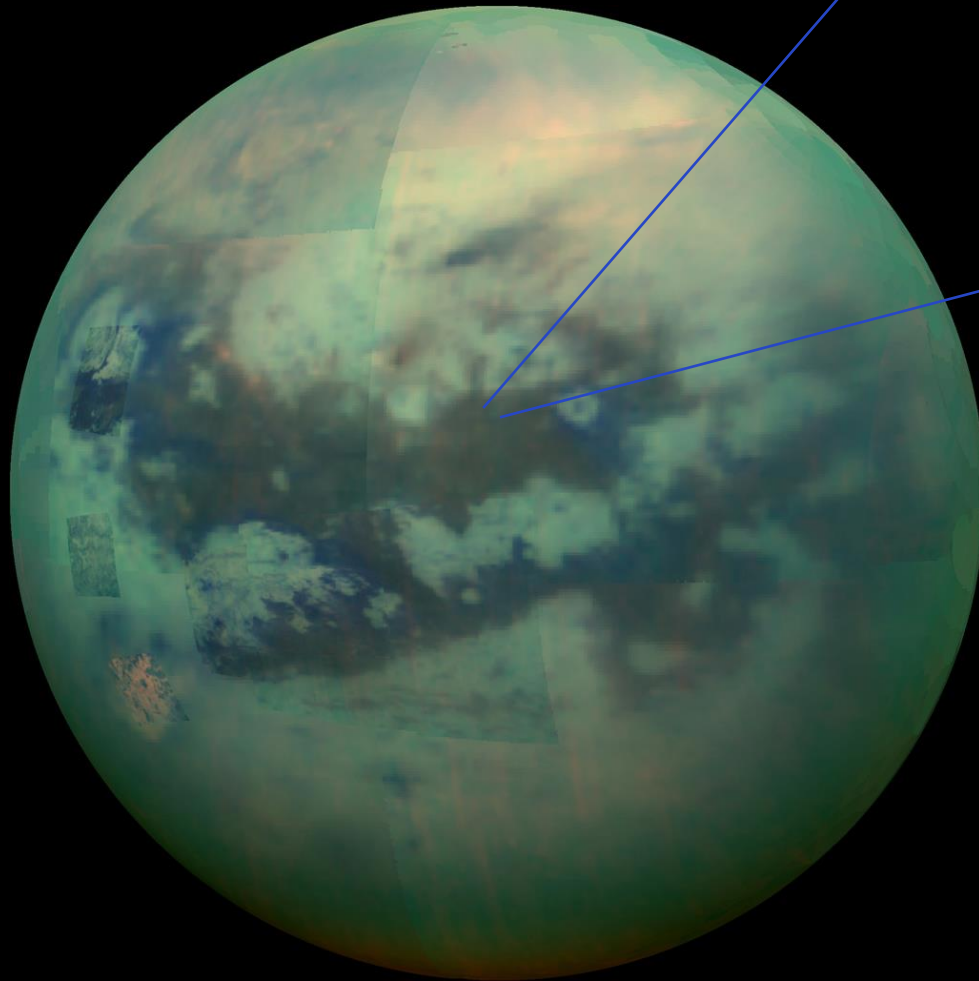| 2 Atoms		3 Atoms		4 Atoms	5 Atoms	6 Atoms	7 Atoms
CH	CP	H_2O	N_2O	NH_3	HC_3N	CH_3OH	CH_3CHO
CN	NH	HCO^+	MgCN	H_2CO	HCOOH	CH_3CN	CH_3CCH
CH^+	SiN	HCN	$H3^+$	HNCO	CH_2NH	NH_2CHO	CH_3NH_2
OH	SO^+	OCS	SiCN	H_2CS	NH_2CN	CH_3SH	CH_2CHCN
CO	CO^+	HNC	AlNC	C_2H_2	H_2CCO	C_2H_4	HC_5N
H_2	HF	H_2S	SiNC	C_3N	C_4H	C_5H	C_6H
SiO	N_2	N_2H^+	HCP	HNCS	SiH_4	CH_3NC	$c-C_2H_4O$
CS	CF^+	C_2H	CCP	$HOCO^+$	$c-C_3H_2$	HC_2CHO	CH_2CHOH
SO	PO	SO_2	AlOH	C_3O	CH_2CN	H_2C_6	C_6H^-
SiS	O_2	HCO	H_2O^+	$l-C_3H$	C_5	C_5S	CH_3NCO
NS	AlO	HNO	H_2Cl^+	$HCNH^+$	SiC_4	HC_3NH^+	HC_5O
C_2	CN^-	HCS^+	KCN	H_3O^+	H_2CCC	C_5N	
NO	OH^+	HOC^+	FeCN	C_3S	CH_4	HC_4H	
HCl	SH^+	SiC_2	HO_2	$c-C_3H$	HCCNC	HC_4N	
NaCl	HCl^+	C_2S	TiO_2	HC_2N	HNCCC	$c-H_2C_3O$	
AlCl	SH	C_3	CCN	H_2CN	H_2COH^+	CH_2CNH	
KCl	TiO	CO_2	SiCSi	SiC_3	C_4H^-	C_5N^-	
AlF	ArH^+	CH_2	S_2H	CH_3	CNCHO	HNCHCN	
PN	NS^+	C_2O	HCS	C_3N^-	HNCNH	SiH_3CN	
SiC		MgNC	HSC	PH_3	CH_3O		
		NH_2	NCO	HCNO	NH_3D^+		
		NaCN		HOCN	H_2NCO^+		
				HSCN	$NCCNH^+$		
				HOOH	CH_3Cl		
				$l-C_3H^+$			
				HMgNC			
				HCCO			
				CNCN			

McGuire 2018

TITAN : ION DETECTION

- Cassini's CAPS-ELS instrument demonstrates the presence positive and negative heavy ions (up to 13 800 amu/q)

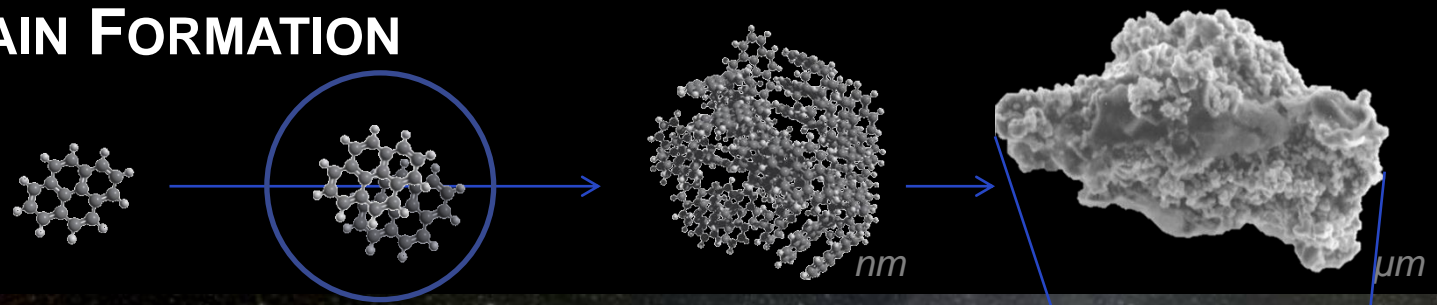- On the basis of a photochemical model, peaks assigned to C_xN^- ions
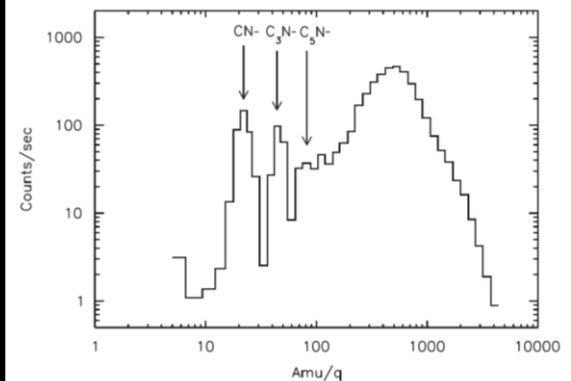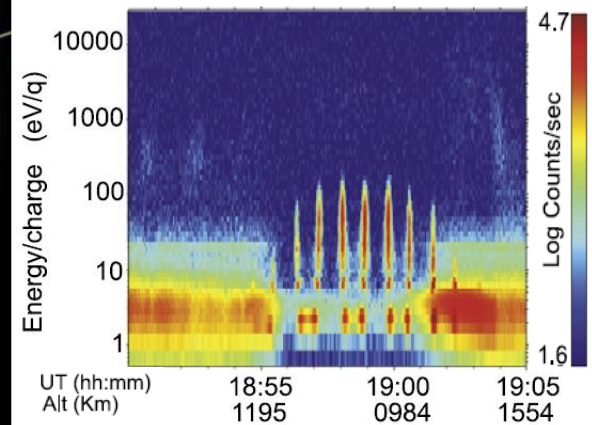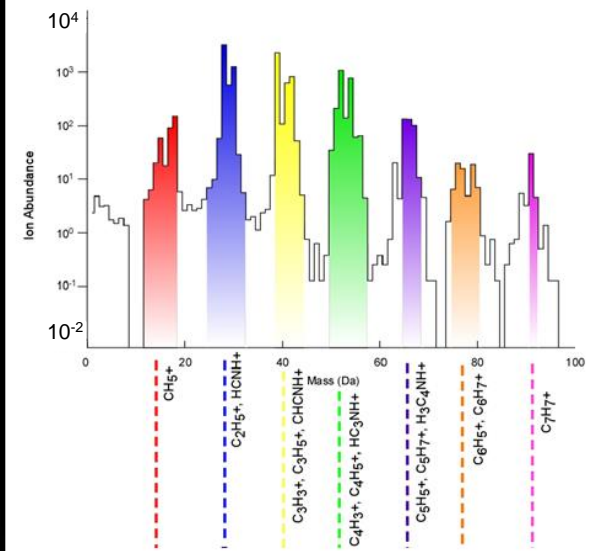
J. H. Waite Jr et al, Science 316, 870 (2007)
A. J. Coates et al, GRL, 34, L22103, (2007)
V.Vuitton et al, Planetary and Space Science57(2009)1558–1572
NASA/JPL-Caltech/Space Science Institute

TITAN AEROSOLS FORMATION

- Expected role in aerosol formation
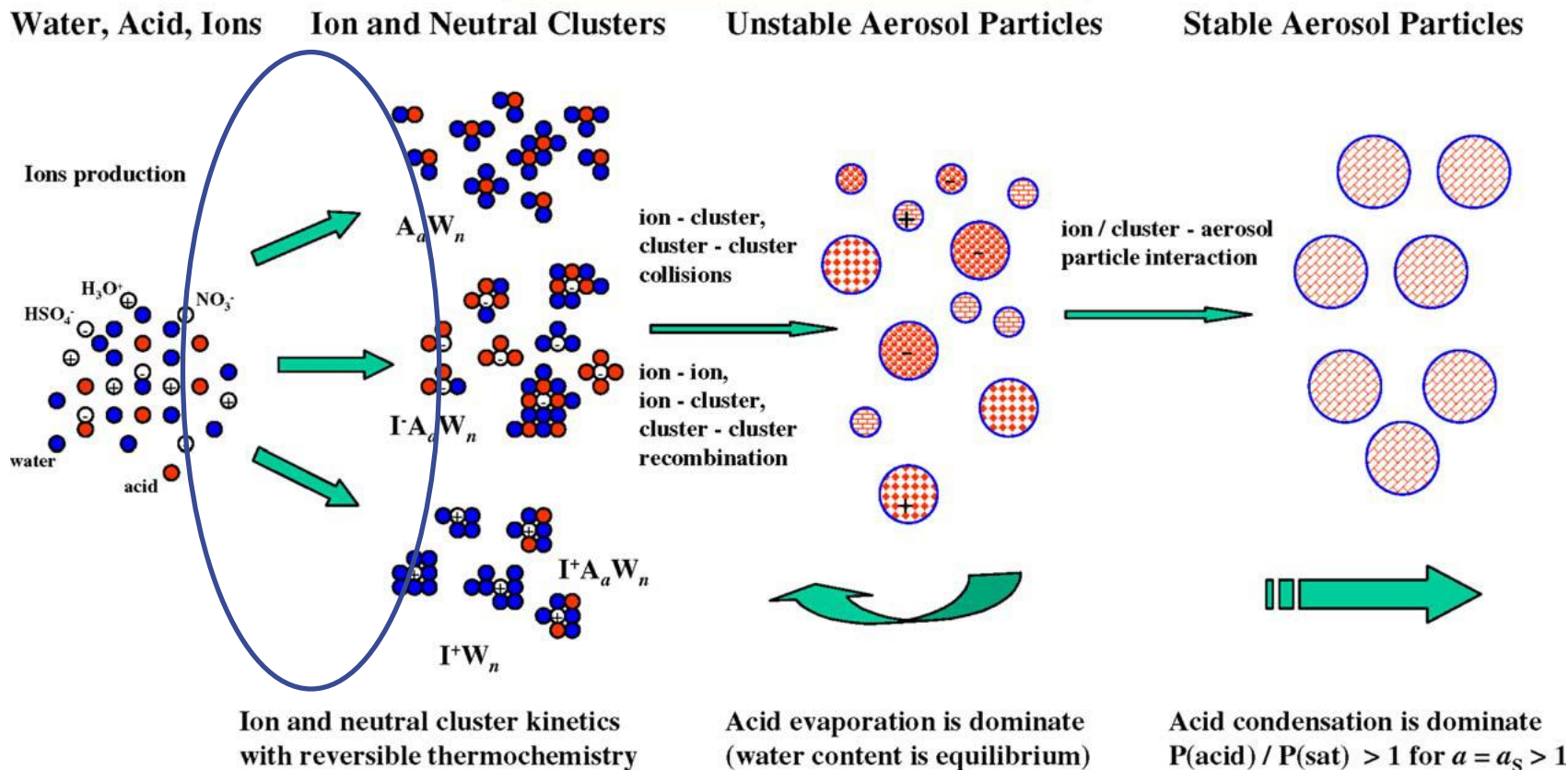- Formation & destruction mechanisms poorly known (low temperature kinetics & products).


Tholin formation in Titan's upper atmosphere

P. Lavvas et al, PNAS, 110, 8, 2729-2734 (2013)
NASA/JPL-Caltech/Space Science Institute

5

2019

DUST GRAIN FORMATION

nm

um

https://www.universetoday.com
Gatchell et al, J. Physics B, 49, 16, 2016

2019

EARTH : AEROSOLS FORMATION

Ion - Cluster - Aerosol Kinetic Model

Water, Acid, Ions   Ion and Neutral Clusters   Unstable Aerosol Particles   Stable Aerosol Particles

Ions production

ion - cluster, cluster - cluster collisions

ion - ion, ion - cluster, cluster - cluster recombination

ion / cluster - aerosol particle interaction

$A_a W_n$

$I^- A_a W_n$

$I^+ A_a W_n$

$I^+ W_n$

Ion and neutral cluster kinetics with reversible thermochemistry

Acid evaporation is dominate (water content is equilibrium)

Acid condensation is dominate $P(acid) / P(sat) > 1$ for $a = a_S > 1$

(i) Kinetics of cluster ions formation for every $a = 1, 2,..., a_S, ...$
(ii) a_S is large, so thermodynamics of (a_S, n)-particle is closed to bulk properties;
(iii) aerosol particles with $a = a_S, a_S+1, ...$ are readly grow;
$(A = H_2SO_4, W = H_2O)$

LABORATORY ASTROPHYSICS
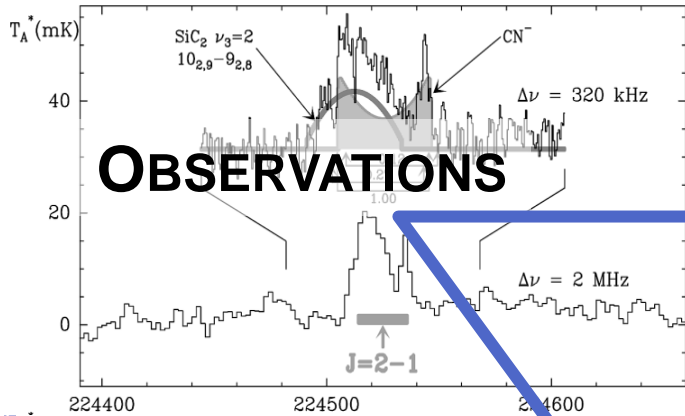
OBSERVATIONS

Agundez & Thaddeus 2010 -AA
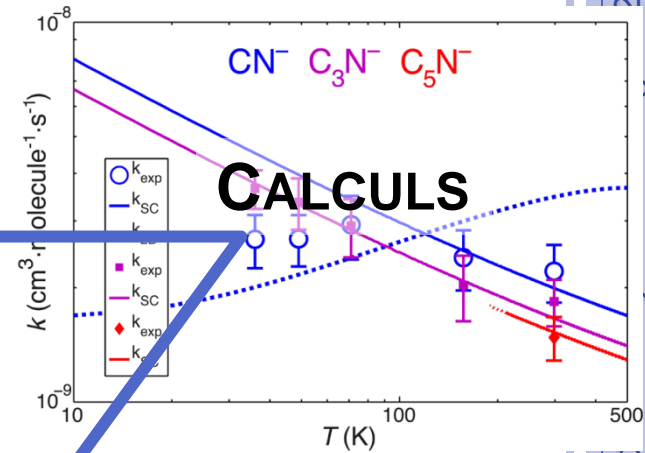
CALCULS

Absolute value of $k_{global}(T)$
And RB(T) measurements:

$$A^{\pm} + B \longrightarrow \text{products}$$
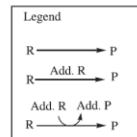$$\longrightarrow \text{products}$$
$$\longrightarrow \dots$$
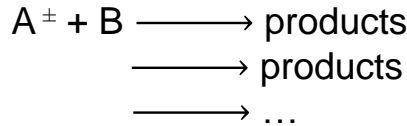
Products (charged) identification
Gas Phase
Low temperature 12K

Experimental kinetic measurements with molecular anions T<150K: less than 10 publications
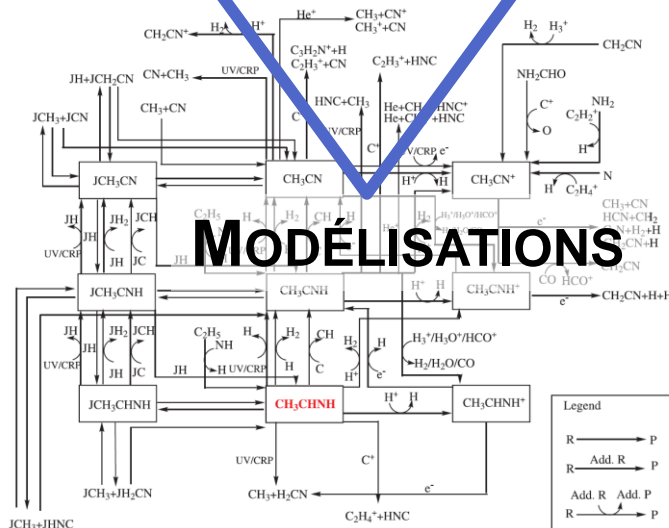
MODÉLISATIONS

Quan & Herbst 2016-ApJ

8

SUMMERY

❑ Reactions
  ❖ Energy considerations
  ❖ Bi-molecular reactions

❑ Rate coefficient
  ❖ Bi-molecular reactions with ions
  ❖ Capture models
  ❖ Temperature dependance, extrapolation

❑ Experimental studies at low temperature
  ❖ Ion traps
  ❖ Cross beams
  ❖ Merged beams
  ❖ Flowing tubes
  ❖ CRESU-SIS

❑ Results with CRESU-SIS method
  ❖ $Ar^+ + N_2$
  ❖ $Ar^+ + C_2H_6$
  ❖ $O_2^+ + C_2H_6$
  ❖ $Ar^+ + N_2O$

9

REACTIONS

02/09/2019

REACTION

- Unimolecular Reaction

$$A \longrightarrow A^* \longrightarrow \text{products}$$
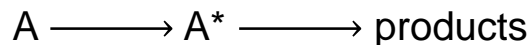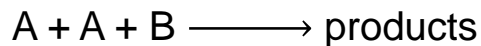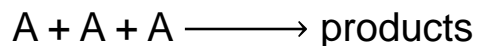
  - Energy barrier
  - Bimolecular with unreactive molecule M induce this reaction
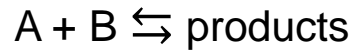 - Photon induced reaction

- Bimolecular Reaction

$$A + A \longrightarrow \text{products}$$
$$A + B \longrightarrow \text{products}$$
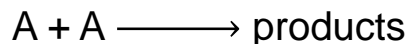
  - Energy barrier or barrierless
  - Anion, cation, neutral, radical

- Termolecular Reaction

$$A + A + A \longrightarrow \text{products}$$
$$A + A + B \longrightarrow \text{products}$$
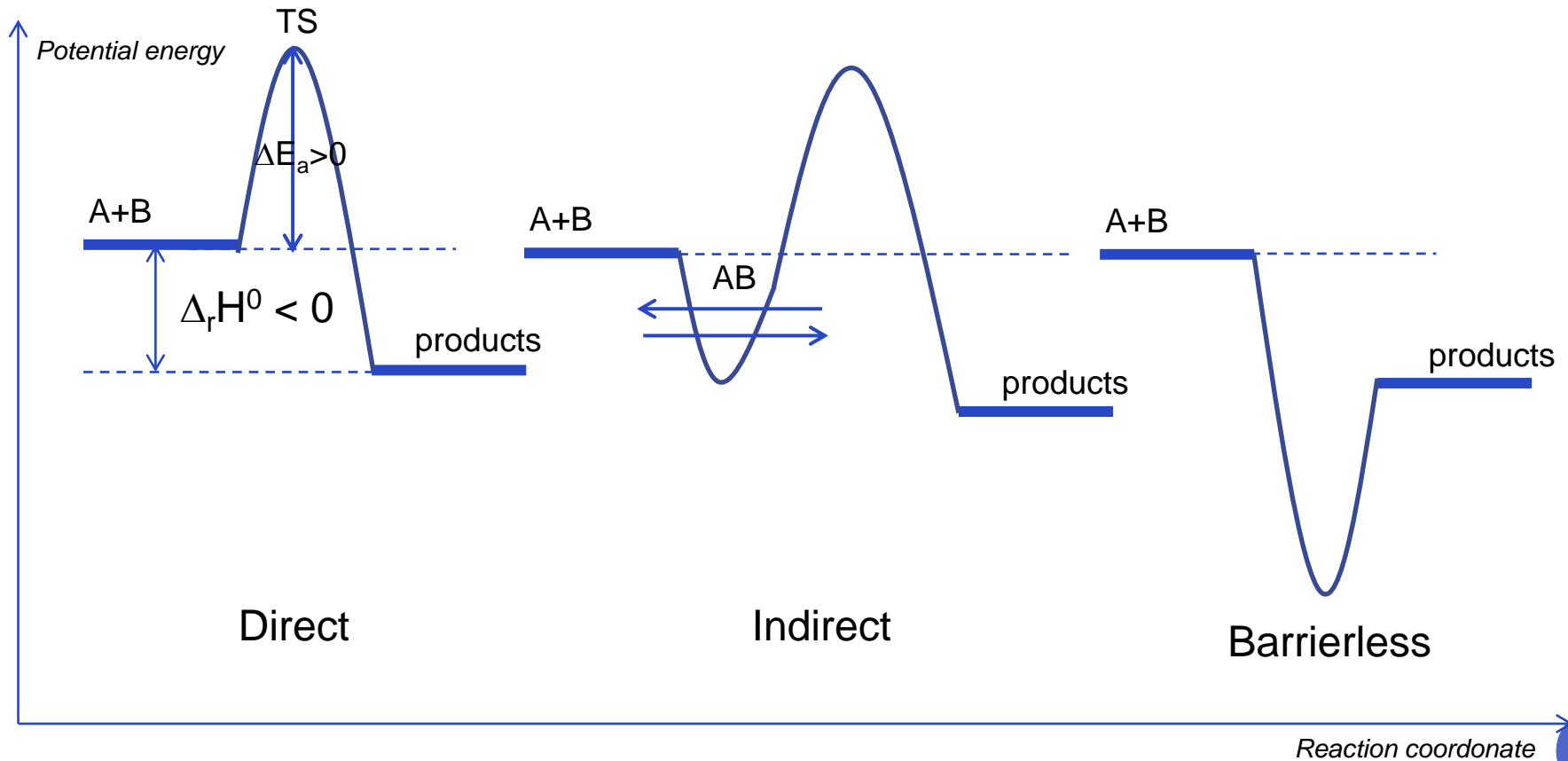$$A + B + C \longrightarrow \text{products}$$
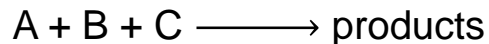
  - Buffer gas cooling
  - Energy transfer in astrophysical environnements
  - Collisional Association reaction

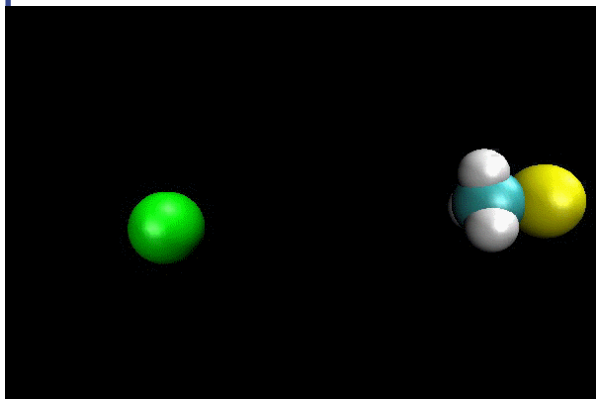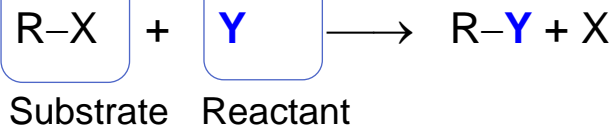# BIMOLECULAR REACTION : ENERGY CONSIDERATIONS

$$A + B \leftrightarrows \text{products}$$

- $\Delta_r H^0 < 0$ ($\Delta_r S^0 > 0$: for T and P constant : $\Delta_r G^0 = \Delta_r H^0 - T\Delta_r S^0$)

Potential energy

TS

$\Delta E_a > 0$

A+B

$\Delta_r H^0 < 0$

products

Direct

A+B

AB

products

Indirect

A+B

products

Barrierless

Reaction coordonate

- Addition (←Elimination) Reactions: A=B   +   **C–D** $\longrightarrow$ CABD* $\xrightarrow{M}$ **C**–A–B–**D**

- Substitution Reactions: R–X   +   **Y** $\longrightarrow$ R–**Y** + X

  Substrate   Reactant
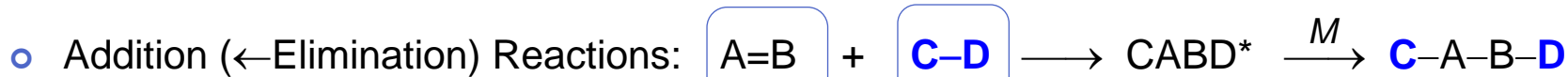
- S_N Nucleophilic reaction, Y = Nu = nucleophile
- S_E Electrophilic reaction, Y = electrophile
- S_R Radical reaction, Y = radical

- $Cl^- + CH_3I \longrightarrow ClCH_3 + I^-$: S_{N2} Reaction, ab initio MP2(fc)/aug-cc-pVDZ/ECP, *High Performance Computing Center, Texas Tech University*
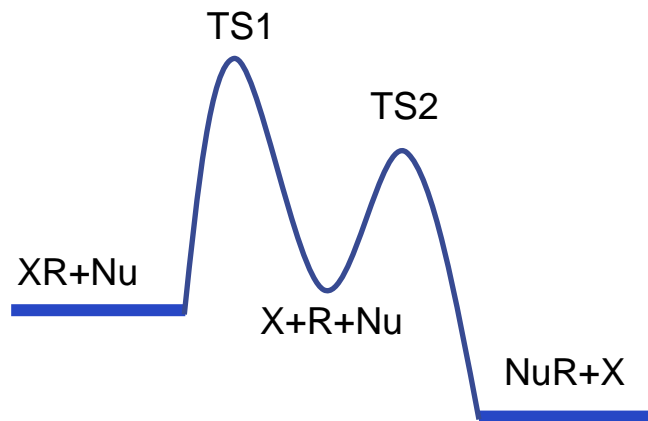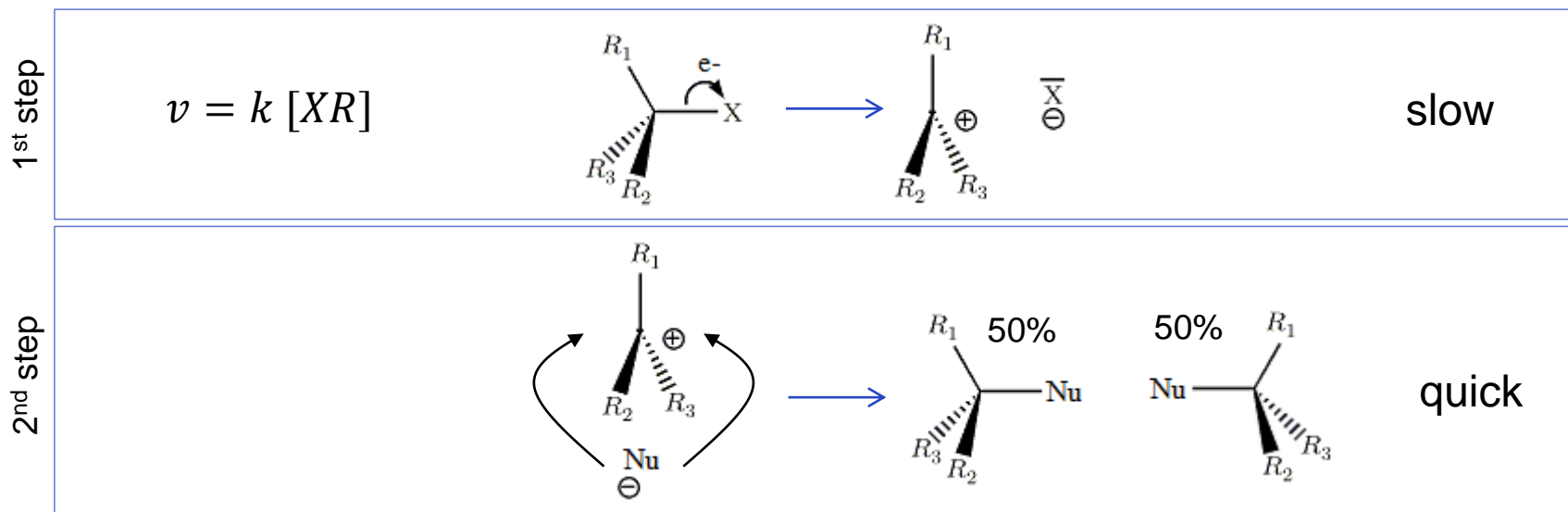
- Oxydo- reduction reaction   Red $\underset{\text{réduction}}{\overset{\text{oxydation}}{\rightleftharpoons}}$ Ox + e
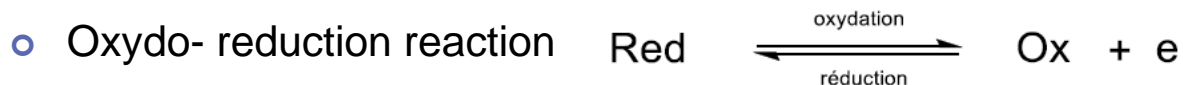
- Rearrangement reaction: isomerization

SUBSTITUTION REACTIONS

- Nu + R$-$X $\longrightarrow$ R$-$Nu + X

- S$_{N1}$: Monomolecular nucleophilic substitution, Y = Nu = nucleophile

1st step

$$v = k\,[XR]$$

slow

2nd step

50%   50%

quick

TS1

TS2

XR+Nu

X+R+Nu

NuR+X

- R$^{\oplus}$ must be stable
- R-X ↗ , X size ↗ $\Longrightarrow$ v ↗
- v is independant of Nu nature but Nu must be more reactive than RX : anion, neutral species with a non-bonding pair H$_2$O; NH$_3$ …
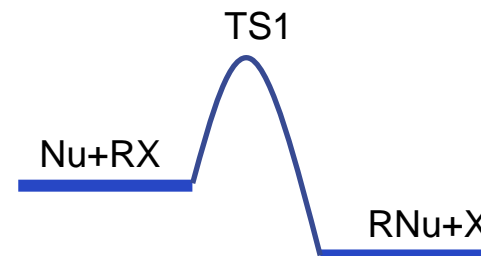
14

SUBSTITUTION REACTIONS

- Nu + R–X $\longrightarrow$ R–Nu + X
- S_{N2}: Bimolecular nucleophilic substitution, Y = Nu = nucleophile

1 step

$$v = k[Nu][XR]$$
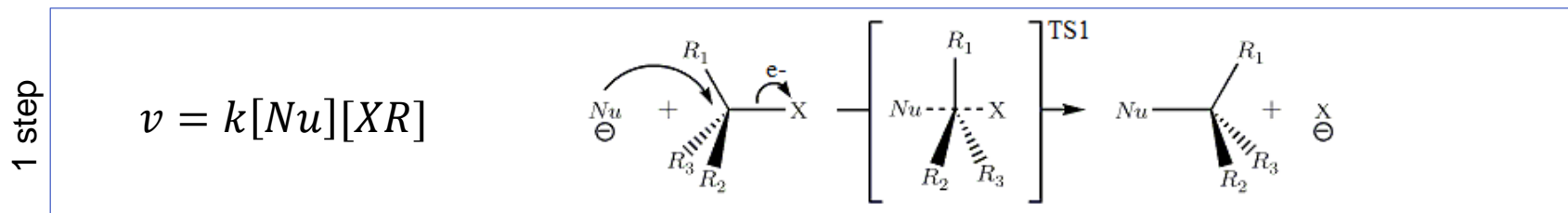
- 1st pseudo order $[Nu] \gg [XR] \Rightarrow v = k\,[XR]$

  ➤ TS1 very instable
  ➤ R-X ↗ , R size ↘ $\Rightarrow v$ ↗
  ➤ Nu size ↘ $\Rightarrow v$ ↗

- Nu⁻ + R–X $\longrightarrow$ Nu⁻···R–X $\longrightarrow$ Nu–R–X⁻ $\longrightarrow$ Nu–R + X⁻
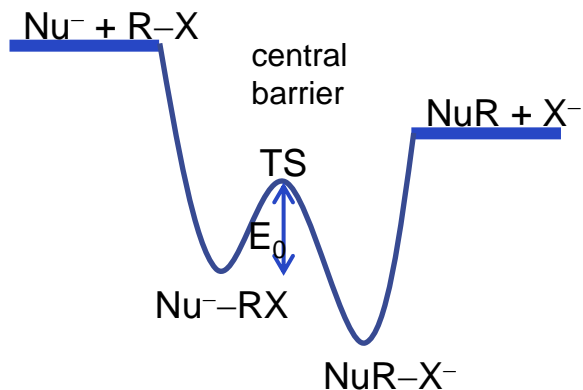
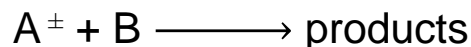Low E_0 : fast reaction will occur
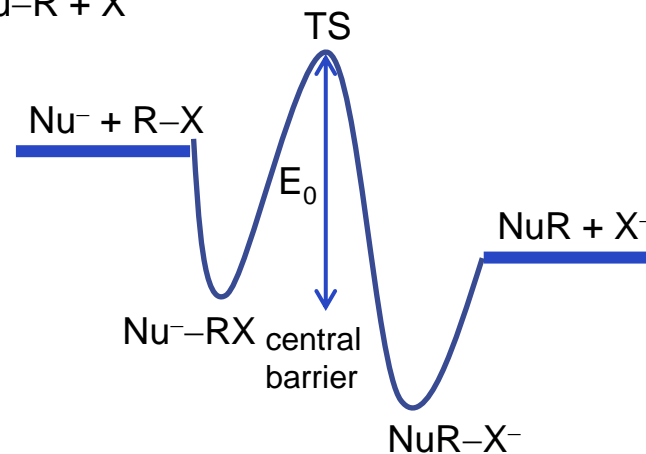
high E_0 : slow reaction will occur

15

Rate Coefficient
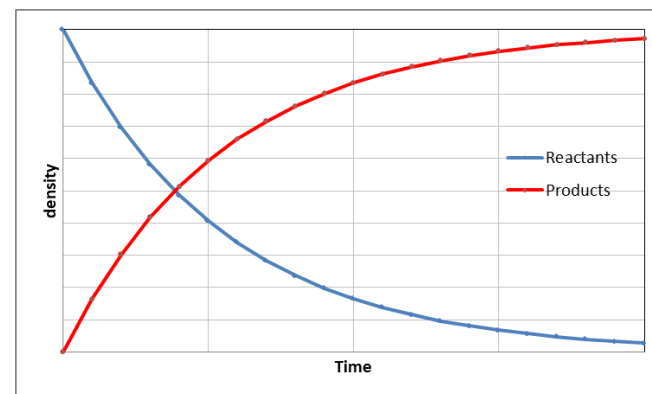
Bi-Molecular Reactions: Kinetic Considerations

- réaction est élémentaire, l'ordre global est aussi la molécularité de la réaction

$$A^{\pm} + B \longrightarrow products$$

- Rate of the reaction :

$$rate = \frac{quantity\ of\ formed\ products}{time} = -\frac{quantity\ of\ transformed\ reactants}{time}$$

measurement of the quantity of material	Rate	units
Mass m	$rate = \frac{\Delta m}{\Delta t}$	g/s
Volume V	$rate = \frac{\Delta V}{\Delta t}$	L/s
Pressure P	$rate = \frac{\Delta P}{\Delta t}$	kPa/s
Molar Concentration C	$rate = \frac{\Delta C}{\Delta t}$	mol/L.s
Number of particules N	$rate = \frac{\Delta N}{\Delta t}$	mol/s
Density [A]	$rate = \frac{\Delta [A]}{\Delta t}$	molecules.cm^{-3}/s

- The rate coefficient is dependant of
  - The reactant & substrate densities
  - The pressure (3th body)
  - The energy barrier
  - The temperature

BI-MOLECULAR REACTIONS: KINETIC CONSIDERATIONS

$$A^{\pm} + B \longrightarrow \text{products}$$
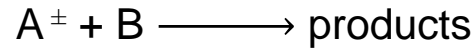
- ○ Kinetic Equation: $\quad \text{rate} = \dfrac{d[A^{\pm}]}{dt} = -k(T)[A^{\pm}][B]$

  - $[A^{\pm}]$, $[B]$ = densities (*molecule.cm^{-3}*) ; *k(T)* = rate coefficient (*molecule^{-1}.cm^3/s*) ; rate (*molecule.cm^{-3}/s*)

- ○ Reaction = collision + modifications of the atomic bounds
  - σ_c = Collision cross section is controled by the long range potential
  - σ_r = Reaction cross section is controled by potential energy surface of the reactants
  - Reaction efficiency = $\dfrac{\sigma_r}{\sigma_{cl}}$

- ○ Empirical Arrhenius Law,
  - thermal **rate coefficient**: $\quad k(T) = Ae^{-E_a/_{RT}}$
  - where A is independant of T
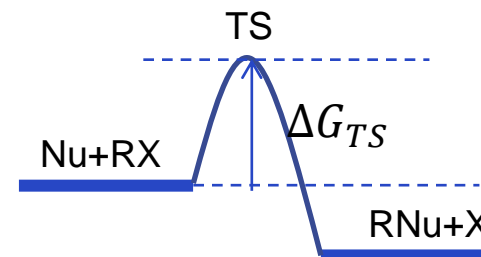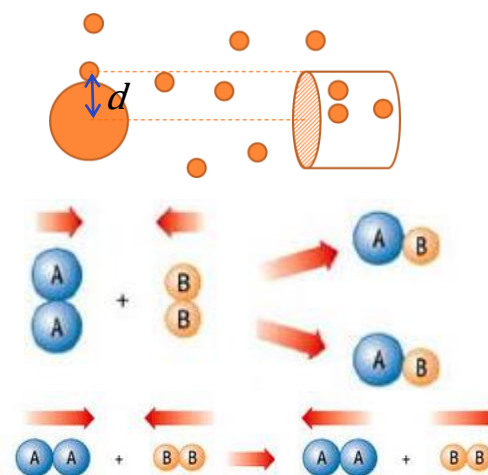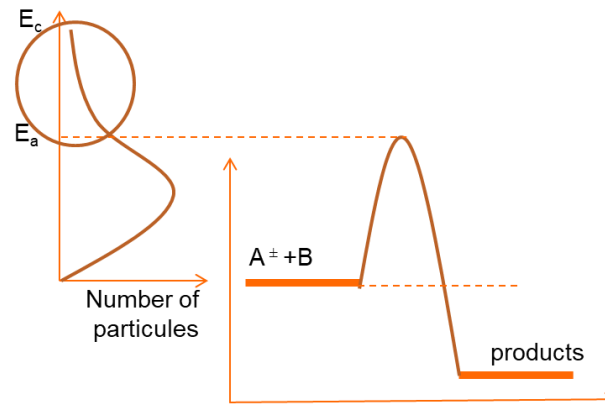
BI-MOLECULAR REACTIONS

- Collision theory :

- $A = P\sigma_c \boxed{\sqrt{\dfrac{8k_BT}{\pi m}}}$ average relative speed

- σ_c , Rigid sphere model: $\sigma_c = \pi(r_A + r_B)^2 = \pi d^2$

- Steric factor P: Hinshelwood:

- Rate coeffcient: $k(T) = P\pi d^2 \sqrt{\dfrac{8k_BT}{\pi m}} e^{-E*/RT}$

- Transition State Theory
  - Non stable Transition State (TS):
  - spontaneous evolution of TS towards products or back to the reactants
  - In equilibrium with the products

$$A^{\pm} + B \leftrightarrows TS \xrightarrow{k\ddagger} products$$

- Rate coefficient: $k(T) = \kappa \boxed{\dfrac{k_BT}{h}} e^{-\Delta G_{TS}/RT}$

$k \ddagger$

02/09/2019

CAPTURE MODELS

○ Rate coefficients:

    • Arrhenius: $\quad k(T) = \boldsymbol{A}e^{-E_a/RT}$ → **no T dependance**

    • Collision Theory: $\quad k(T) = \boldsymbol{P\pi d^2}\sqrt{\dfrac{8k_BT}{\pi m}}\, e^{-E*/RT}$ → $\boldsymbol{\sqrt{T}}$ **dependance**

    • Transition State Theory: $\quad k(T) = \boldsymbol{\kappa}\dfrac{\boldsymbol{k_BT}}{\boldsymbol{h}}\, e^{-\Delta G_{TS}/RT}$ → **T dependance**
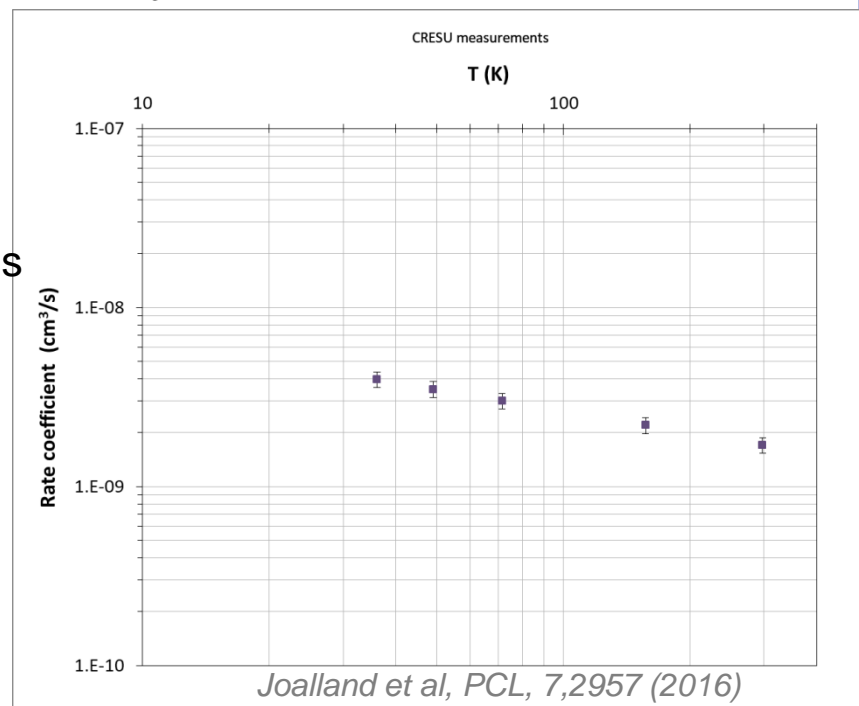
○ Theory Limitations:
    • Rigid spheres (no P modelisation)
    • Bimolecular reactions

○ Evolution Collision theory = Capture models
    • Polarizability
    • Dipole moment
    • Orientation of the dipole moment

$C_3N- + HCOOH \rightarrow$ products

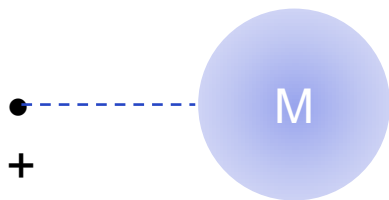
Joalland et al, PCL, 7,2957 (2016)

LANGEVIN MODEL (LANGEVIN 1905 + GIOMOUSIS ET STEVENSON 1958)

- Interaction between an ion (charged point) and a neutral **non polar** molecule M (sphere)

$$V_L = V_{eff}(r) = E_{rot}(r) + U(r) = \frac{L^2}{2mr^2} - \frac{\alpha e^2}{2r^4} = \boxed{\frac{mv^2}{2}} \cdot \frac{b^2}{r^2} - \boxed{\frac{\alpha e^2}{2r^4}}$$
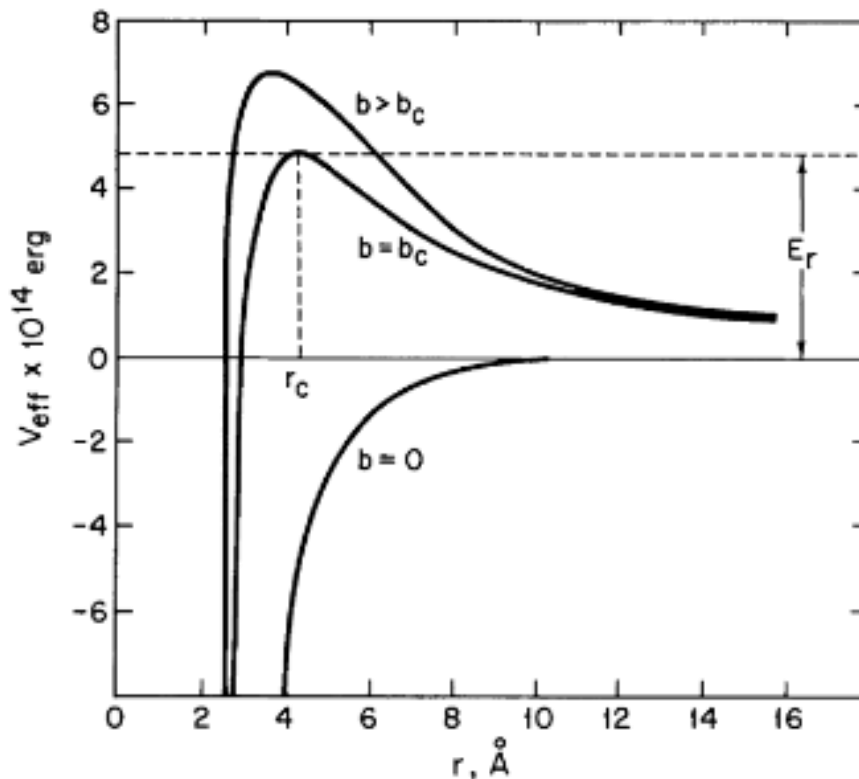
Relative impact (translational) energy E_r

Classical electrostatic attractive potential ion-neutral

- When b = 0 the ion is attracted directly and reacts

- When b ≠ 0 : centrifugal barrier !
- $b = b_c$, $V_{eff}(r_c)$ max :

$$r_c = \frac{1}{4}\sqrt{\frac{\alpha e^2}{E_r}} \rightarrow V_{eff}(r_c) = \frac{E_r^2 b_c^4}{2\alpha e^2}$$

$$V_{eff} = E_r \rightarrow \boxed{b_c = \left(\frac{2\alpha e^2}{E_r}\right)^{\frac{1}{4}}} \rightarrow \sigma_L = \pi e\sqrt{\frac{2\alpha}{E_r}}$$

P. M. Langevin, Ann. Chem. Phys.**5**, 245 (1905).G. Gioumousis and D. P. Stevenson, J. Chem. Phys.**29**, 294 (1958)

LANGEVIN MODEL

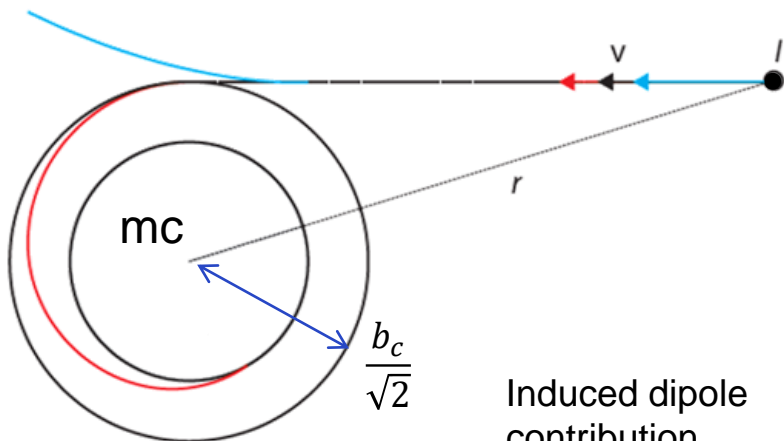$$V_{eff}(r) = -\frac{\alpha e^2}{2r^4} + \frac{mv^2}{2} \cdot \frac{b^2}{r^2}$$

- When $b > b_c$ the capture collision probability is 0
- When $b = b_c$ the ion / molecule orbit around the mc
- When $b < b_c$ the capture collision probability is 1

With centrifugal barrier

$$b_c = \left(\frac{2\alpha e^2}{E_r}\right)^{\frac{1}{4}}$$

mc

$\frac{b_c}{\sqrt{2}}$

Induced dipole contribution

$$\sigma_L = \pi b_c^2 \Rightarrow k_L = \sigma_L v \Rightarrow \boxed{k_L = 2\pi e \sqrt{\frac{\alpha}{m}}}$$

- Only long range interaction
- $E_r < 1eV$
- The structure and the chemical and physical properties of the molecules are not taken into account.
- Works well for ions compared with radicals (due to the lower attractive forces in action). Long range attraction may not be valid compared to short range

22
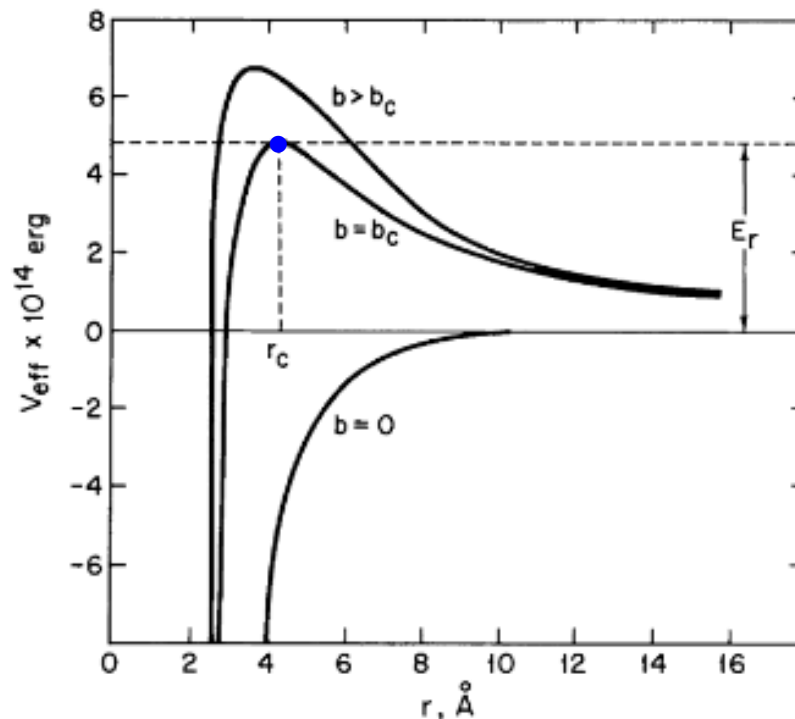
LOCKED DIPOLE MODEL (GIOUMOUSIS, STEVENSON 1958, THEARD, MORAN, HAMILL 1963)

- Interaction between an ion (charged point) and a neutral molecule (sphere) with a **permanent dipole** $\vec{\mu}$:
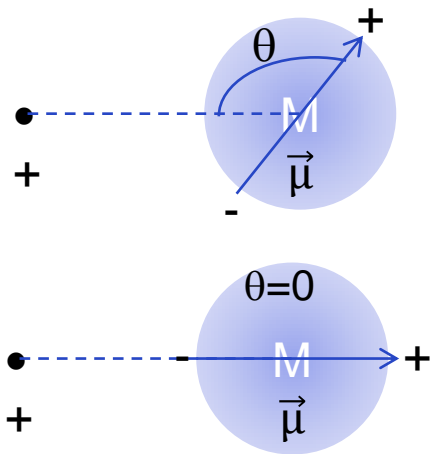
- If no alignment of the dipole with the incoming charge, the interaction averages to zero and Langevin theory is applied: V_L

- If the molecule dipole "locks-in" as the ion approaches, then the ion-dipole interaction is taken into consideration: V_{LD}

$$V_{LD}(r) = V_L - \frac{e\mu}{r^2} == \frac{mv^2}{2} \cdot \frac{b^2}{r^2} - \frac{\alpha e^2}{2r^4} \boxed{- \frac{e\mu}{r^2}}$$

- Rate coefficient for thermal ions

$$\boxed{k_{LD} = k_L + 2\pi e \frac{\sqrt{2}\mu}{\sqrt{m\pi k_B T}}}$$

- the dipole effect is overestimated in this model ← the ion field doesn't completely quench the rotational angular momentum of the polar molecule.

- k_B is Boltzmann's constant = 1,3806$10^{-16}$ erg.K^{-1} (cgs)
- T is the absolute Temperature

T. F. Moran and W. H. Hamill, J. Chem. Phys. 39, 1413 (1963)

AVERAGE DIPOLE ORIENTATION MODEL ADO (SU & BOWERS 1973,79)

o Interaction between an ion (charged point) and a neutral molecule (sphere) with a **permanent dipole** $\vec{\mu}$ (average orientation).
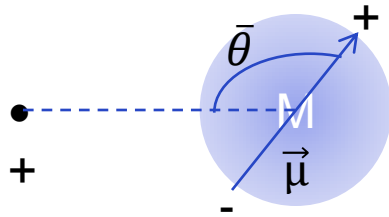
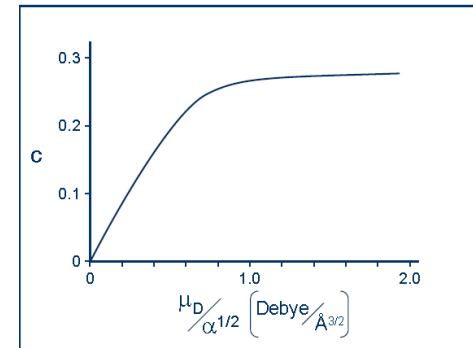$$V_{LD}(r) = V_L - \boxed{\frac{e\mu\cos(\bar{\theta}(r))}{r^2}}$$

Average dipole energy

o Predicts the dipole dependence in proton transfer, charge transfer, and momentum transfer collisions.

$$\boxed{k_{ADO} = k_L + 2\pi e \frac{C\sqrt{2}\mu}{\sqrt{m\pi k_B T}}}$$

o No net angular momentum between the rotating molecule and the ion-molecule orbital motion (not conserved, oscillations)

o $\mu\nearrow$ locking of the dipole $\nearrow$

- T=constante, $C = f(\mu/\sqrt{\alpha})$ is the dipole locking constant:
  - o The effectiveness of locking the dipole
  - o Qualitatively considered as cos<θ> where <θ> is the average orientation angle of the dipole.
- For $E_r < 0.1 eV$

o Bass et al (1975) → $\overline{\cos(\theta)}$

24

T. Su and M. T. Bowers, J. Chem. Phys.58, 3027 (1973) ; L. Bass, T. Su, W. Chesnavich, and M. T. Bowers, Chem. Phys. Lett.34, 119 (1975)

ANGULAR MOMENTUM CONSERVED AADO (SU & CHESNAVICH 1978)

- Couple rotational angular momentum of the dipole (J) to orbital angular momentum of the system (L): $\vec{L}$ and $\vec{J}$ are collinear
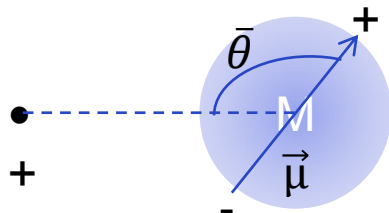
$$V_{LD}(r) = V_L - \frac{e\mu \cos(\bar{\theta}(r))}{r^2}$$

- Rate coefficient:

$$\boxed{k_{SC} = k_L \times G(x)}$$

$$x = \frac{m}{\sqrt{2\alpha k_B T}}$$

- there is a net angular momentum transfer between the rotating molecule and the ion-molecule orbital motion.

- $x < 2 \Rightarrow G(x) = 0.9754 + \frac{(x+0.509)^2}{10.526}$
- $x \geq 2 \Rightarrow G(x) = 0.6200 + (x \times 0.4767)$
- empirical parametrization
- $G(x) < 1$: the dipole moment increase k_L

- $k_{SC} > k_{ADO}$
- Underestimation of the rate coefficient at the lowest temperatures (Marquett et al 1985, Clary et al 1985)
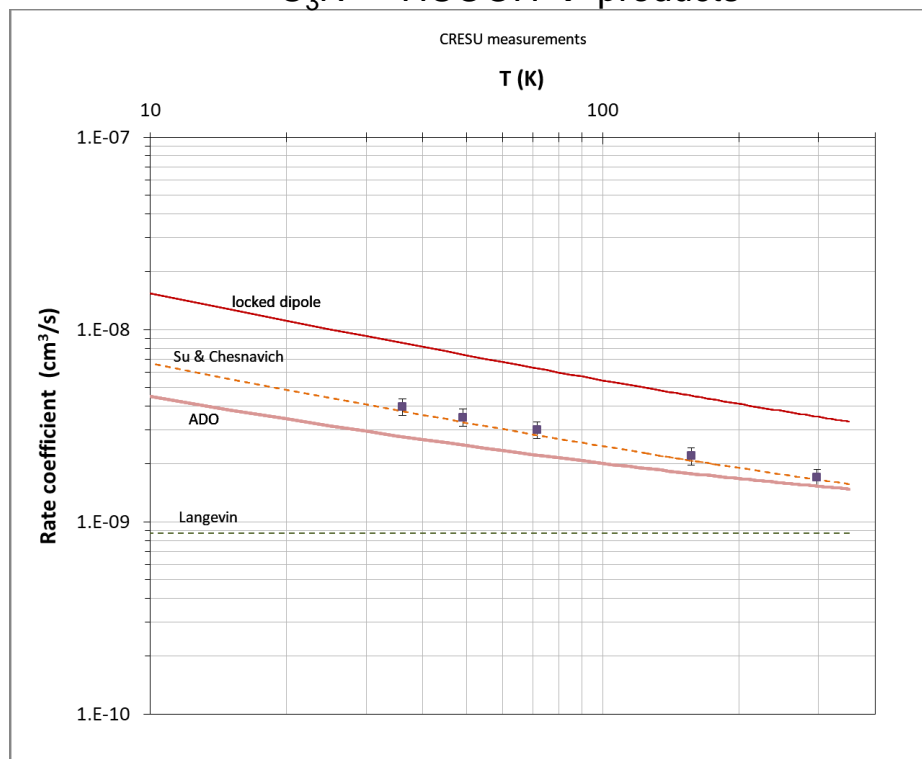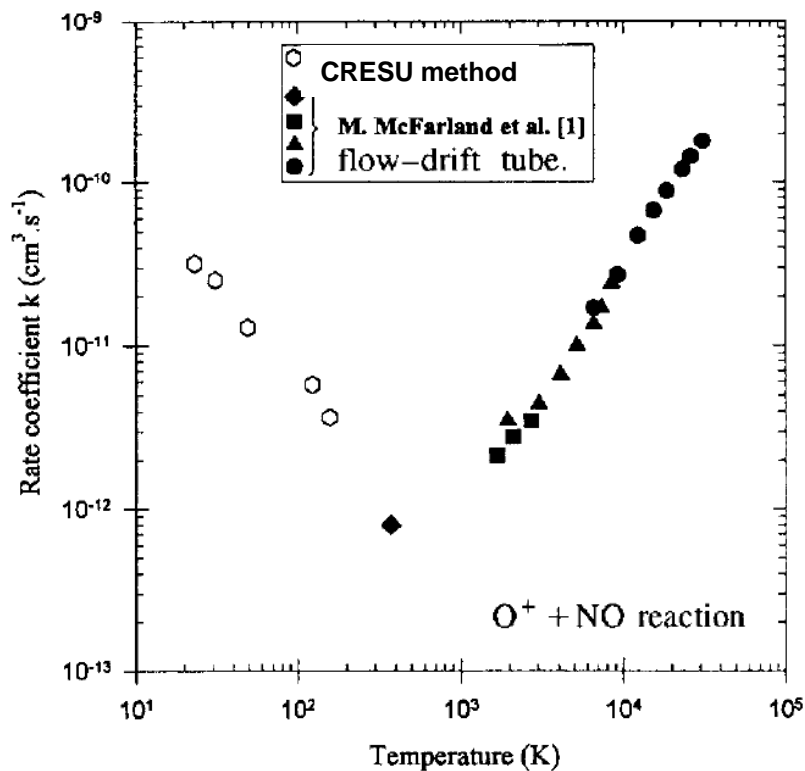
02/09/2019

CAPTURE MODELS: SUMMERY

Langevin	Locked dipole	ADO	Su & Chesnavich
$k_L = 2\pi q \sqrt{\dfrac{\alpha}{m}}$	$k_{SC} = k_L \times x$	$k_{ADO} = k_L \times Cx$	$k_{SC} = k_L \times G(x)$
• Polarizability of neutral reactant	• Polarizability of neutral reactant • Dipole of the neutral reactant: perfect orientation	• Polarizability of neutral reactant • Dipole of the neutral reactant: average orientation • Empirical parametrisation	• Polarizability of neutral reactant • Dipole of the neutral reactant: average orientation • $\vec{L}$ and $\vec{J}$ coupling
• No T dependance	• $\sqrt{T}$ dependance	• $\sqrt{T}$ dependance	• $\sqrt{T}$ or T dependance

02/09/2019

RATE COEFFICIENT

C$_3$N- + HCOOH → products

- C$_3$N- + HCOOH →
  - μ(C$_3$N-) = 3.1 D
  - μ(HCOOH) = 1.41 D
  - α(HCOOH) = 3.32 Å^3

- Extrapolation: is it a good idea ?

- Then we need experimental measurements !
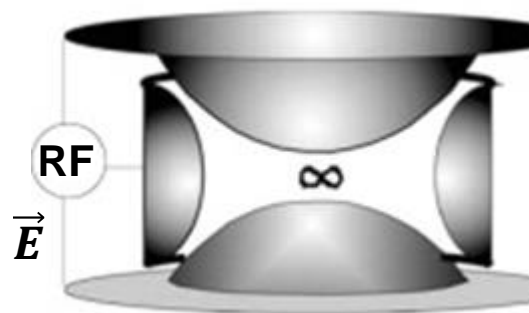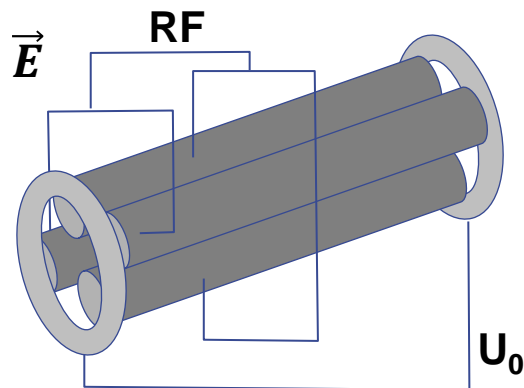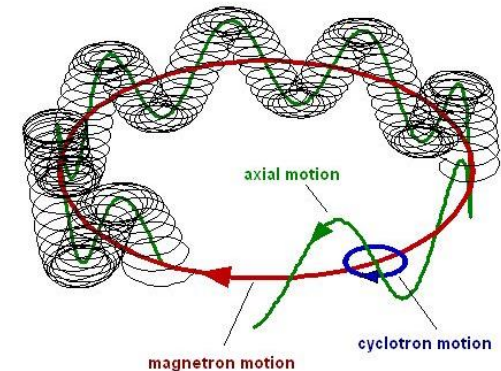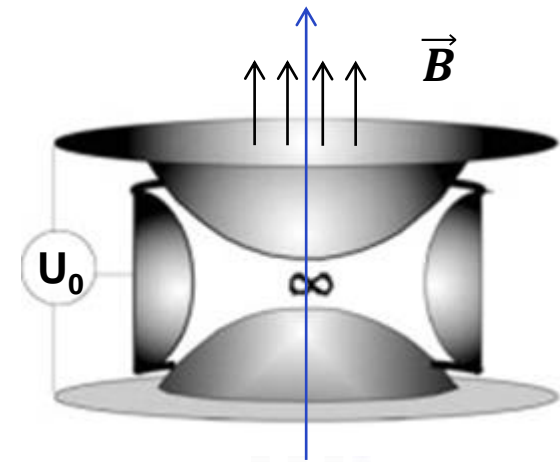
EXPERIMENTAL STUDIES AT LOW TEMPERATURE

ION TRAPS : COLD IONS (≤ FEW K)

➤ low number of particles achievable 10^5-10^6
➤ **longer observation times (min, hours)**

➤ Penning trap: $\vec{B}(\vec{r}, t)\ \vec{E}(\vec{r}, t)$
  • Uniform $\vec{B}$: lateral trapping
  • U_0: axial trapping

➤ Paul trap: $\vec{E}(\vec{r}, t)$ *time dependance*
  • Inhomogeneous electric fields (RF): radial trapping
  • Stability parameter $\eta = \frac{2q|\nabla \vec{E_0}|}{m\Omega_{MHz}{}^2} < 0.3$
  • Additional Static voltages (DC): axial trapping

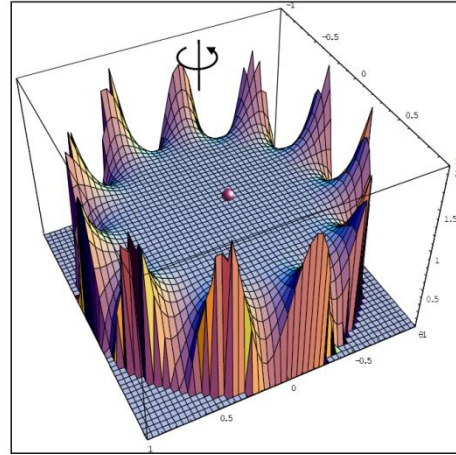*J.D. Siverns et al, Applied Physics B · June 2011, thèse Delahaye Pierre 2002*
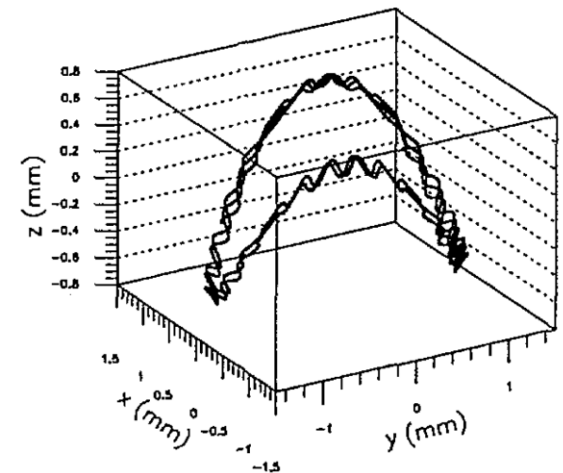
ION TRAPS : COLD IONS (≤ FEW K)

- Linear higher-order multipole RF trap: 22-poles trap (Gerlich)

Quadrupole
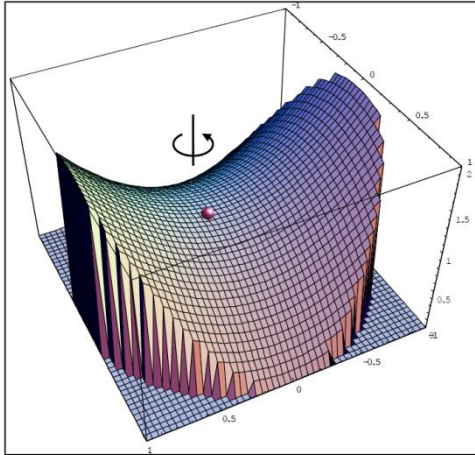
22-Pole

High-order multipole traps offer a large field-free region in the trap center, and therefore provide a reduced interaction time of the ions with the oscillating electric field compared to a quadrupole trap
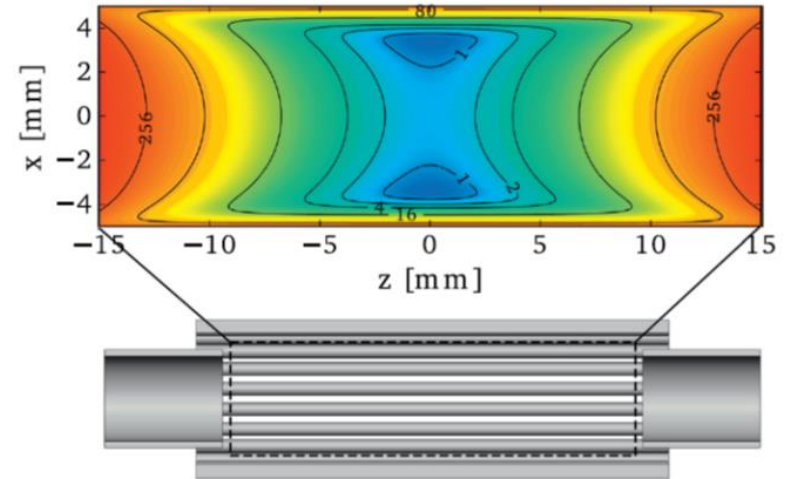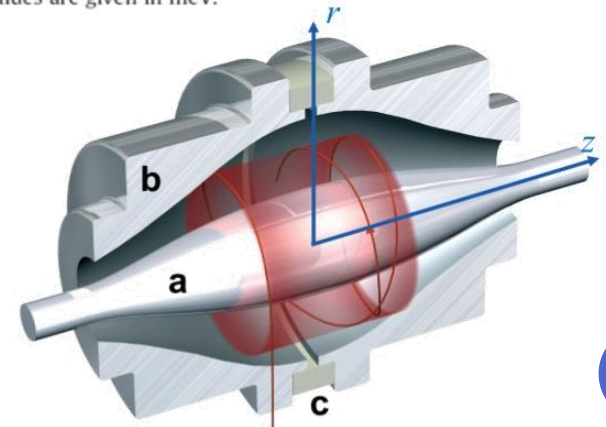
Fig. 8. Lower part: Cross section of a CAD-model of a 22-pole trap including cylindrical end electrodes. Upper part: Effective potential in the x-z-plane. Equipotential values are given in meV.

- Orbitrap

Orbitrap Mass Analyzer – Overview and Applications in Proteomics.
Michaela Scigelova and Alexander Makarov

02/09/2019

ION TRAPS : COLD IONS

- Ion trap + Buffer gas cooling (He,): T 1mTorr, → few K (10K, RF heating):
  - High $\sigma_{elastic\ collision}$ → efficiency
  - Low $\sigma_{inelastic\ and\ reactive\ collision}$
  - $M_{buffer\ gas} < M_{ion}$ → RF heating

- Ion trap + Laser cooling (Doppler effect):
  - atoms → mK > T → µK (Coulomb crystal)

Paul ion trap

Aarhus University
Institut for Fysik og Astronomi

- Ion trap + Sympathetic cooling: atoms and molecules (large). Laser cooled atoms as coolant → bi-component Coulomb crystals
  - Kinetic energy is lost by elastic collisions
  - Finaly, laser cooling

$m_a / m_i = 0.15$
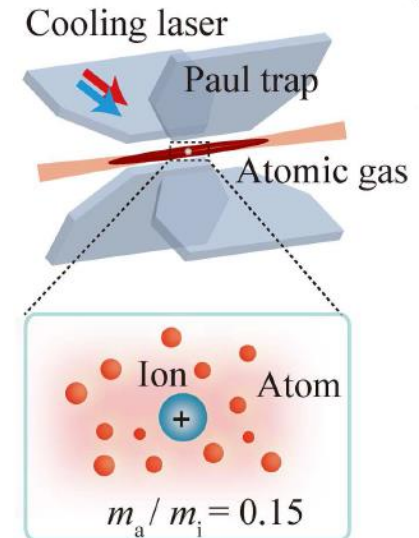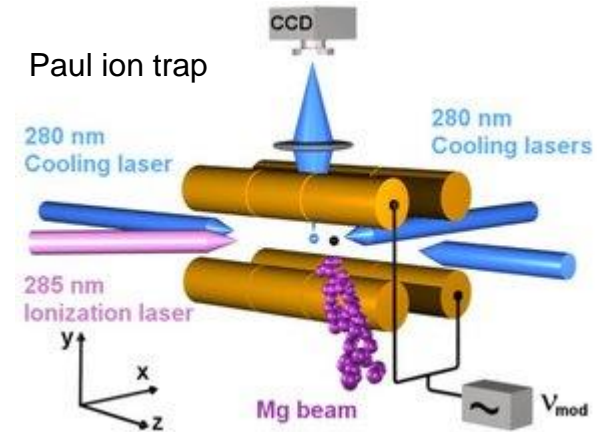
Haze et al, Phys. Rev. Lett. 120, 043401 (2018)

31

CRYOGENIC ION TRAP ILLUSTRATION

CHEMISTRY

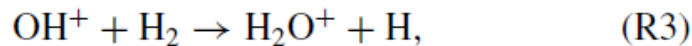## Low temperature rates for key steps of interstellar gas-phase water formation

Sunil S. Kumar[1]*[†], Florian Grussie[1], Yury V. Suleimanov[2,3†], Hua Guo[4], Holger Kreckel[1†]

The gas-phase formation of water molecules in the diffuse interstellar medium (ISM) proceeds mainly via a series of reactions involving the molecular ions OH^+, H_2O^+, and H_3O^+ and molecular hydrogen. These reactions form the backbone for the chemistry leading to the formation of several complex molecular species in space. A comprehensive understanding of the mechanisms involved in these reactions in the ISM necessitates an accurate knowledge of the rate coefficients at the relevant temperatures (10 to 100 K). We present measurements of the rate coefficients for two key reactions below 100 K, which, in both cases, are significantly higher than the values used in astronomical models thus far. The experimental rate coefficients show excellent agreement with dedicated theoretical calculations using a novel ring-polymer molecular dynamics approach that offers a first-principles treatment of low-temperature barrier-less gas-phase reactions, which are prevalent in interstellar chemical networks.

$$H^+ + O \rightarrow O^+ + H, \quad (R1)$$

$$O^+ + H_2 \rightarrow OH^+ + H, \quad (R2)$$

$$OH^+ + H_2 \rightarrow H_2O^+ + H, \quad (R3)$$

$$H_2O^+ + H_2 \rightarrow H_3O^+ + H, \quad (R4)$$

$$H_3O^+ + e \rightarrow OH + H_2, \quad (R5)$$

$$H_3O^+ + e \rightarrow H_2O + H. \quad (R6)$$
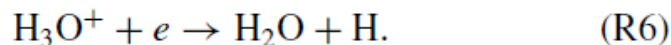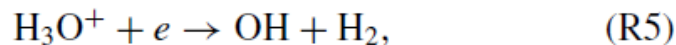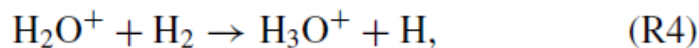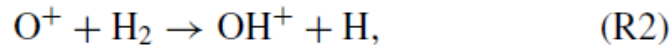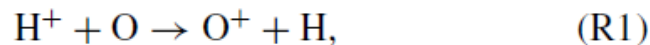
✪ All 3 molecular ions, OH+, H_2O+, and H_3O+, have been observed in the ISM, often in surprisingly high abundance.

✪ No experimental data at low T.

INTERSTELLAR GAS-PHASE WATER FORMATION

Fig. 1. Exemplary ion counts of OH⁺ and H₂O⁺ as a function of storage time and loss rates versus H₂ density. (**Left**) Decay curves of OH⁺ and H₂O⁺ as observed in the 22-pole trap at 21 K with a H₂ number density of 3.2×10^{10} cm^{-3}. The inset shows a spectrum of a typical initial mass distribution produced by the ion source. (**Right**) Loss rates for OH⁺ and H₂O⁺ as a function of H₂ density at two different temperatures. The data points at the lowest densities resulted from the residual H₂ in the trap, which varied with trap conditions and temperature. Those points, while fully consistent with the trend, were not included in the fit.

INTERSTELLAR GAS-PHASE WATER FORMATION

Fig. 2. Comparison of the present measured and calculated rate coefficients for the reactions of OH⁺ and H₂O⁺ with H₂ and previous measurements, QCT calculations, and the Langevin rate coefficient. For the present experimental work and the SIFT results of 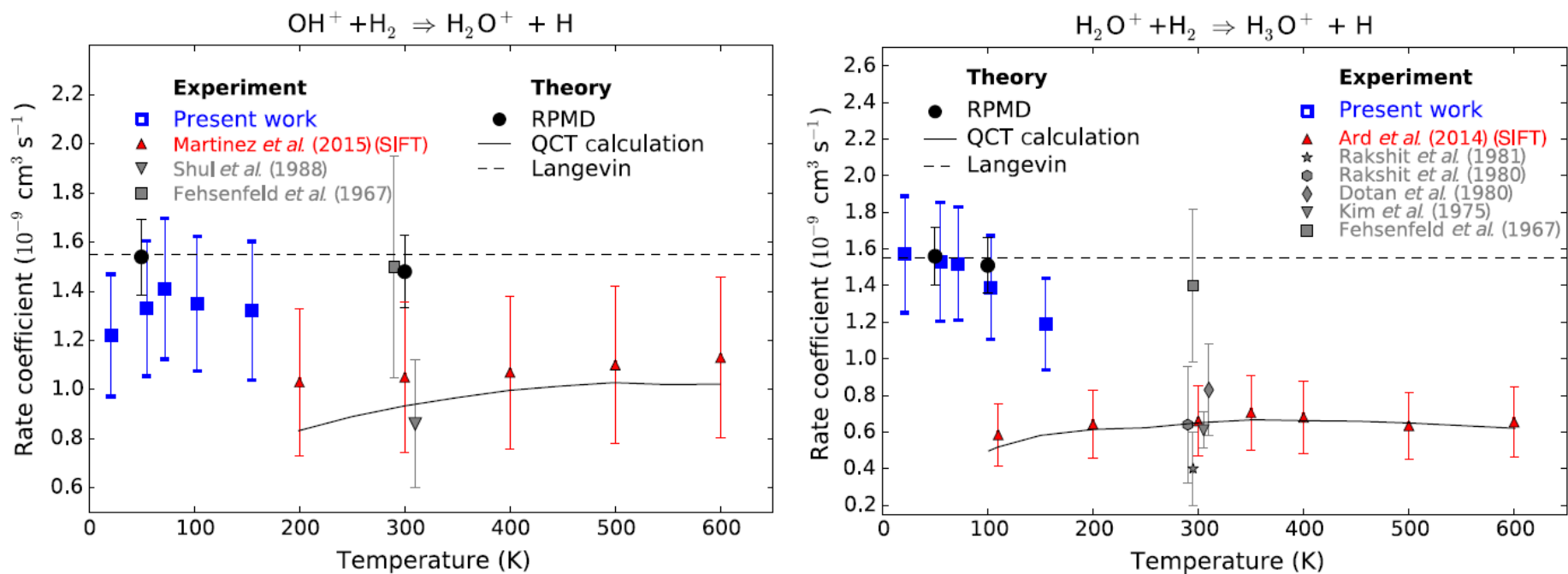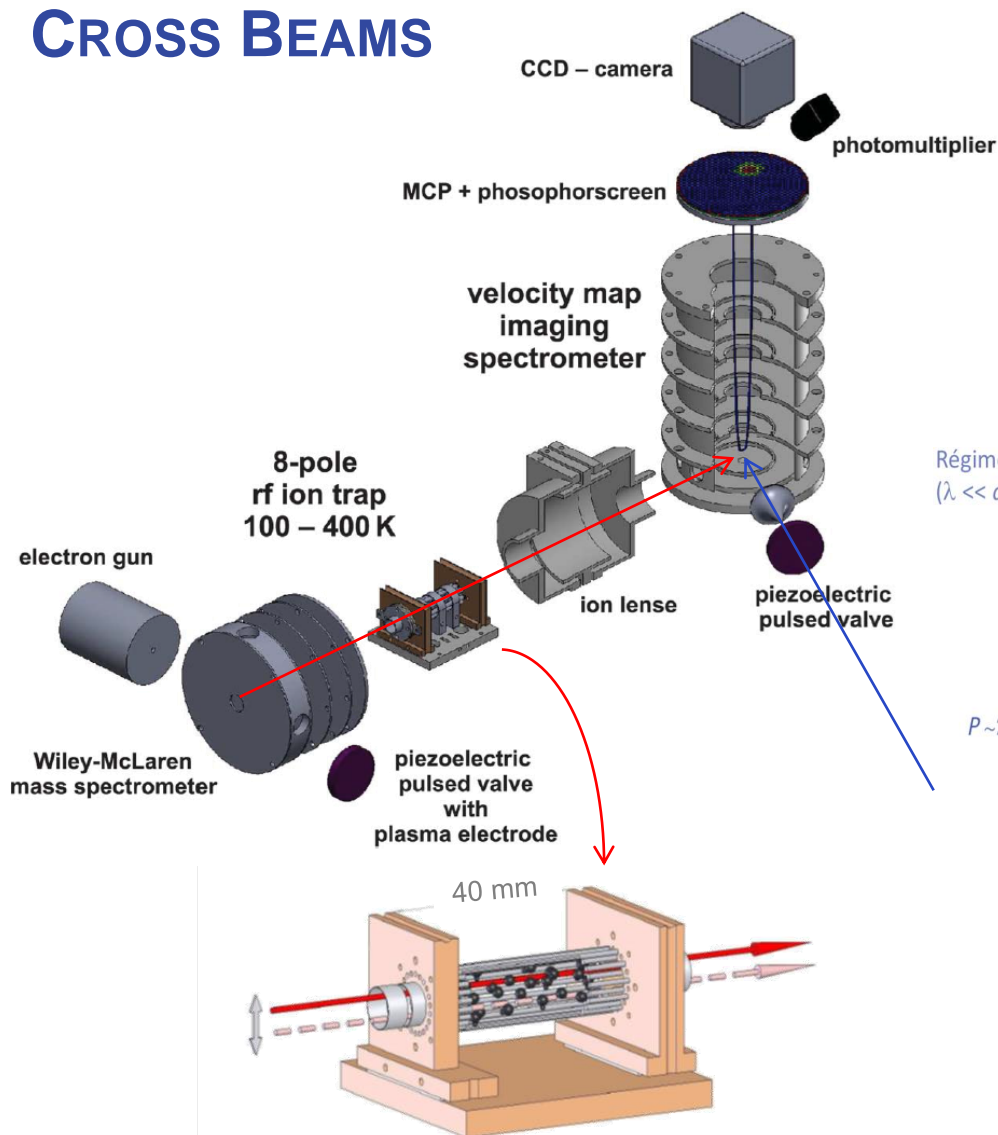(21) and (22), we added the respective relative and absolute uncertainties in quadrature to depict absolute uncertainties for a fair comparison. The uncertainties for the present RPMD calculations represent the convergence limit within two SDs. Also shown are previous room temperature measurements; for clarity, they are shifted in steps of 10 K. Theoretical calculations (RPMD and QCT) were performed using potential energy surfaces (PESs) from (26, 36). References for previous room temperature data are as follows: Shul et al. (1988) (16), Fehsenfeld et al. (1967) (17), Rakshit et al. (1981) (18), Rakshit et al. (1980) (14), Dotan et al. (1980) (20), and Kim et al. (1975) (19). Note that the measurements of Dotan et al. are actually energy-resolved, extend to kinetic center-of-mass collision energies of up to 0.3 eV (corresponding to $k_BT = 3500$ K), and show a slow monotonic decrease. Since the present work is concerned primarily with the low-temperature regime, we only show their lowest energy data point for clarity.
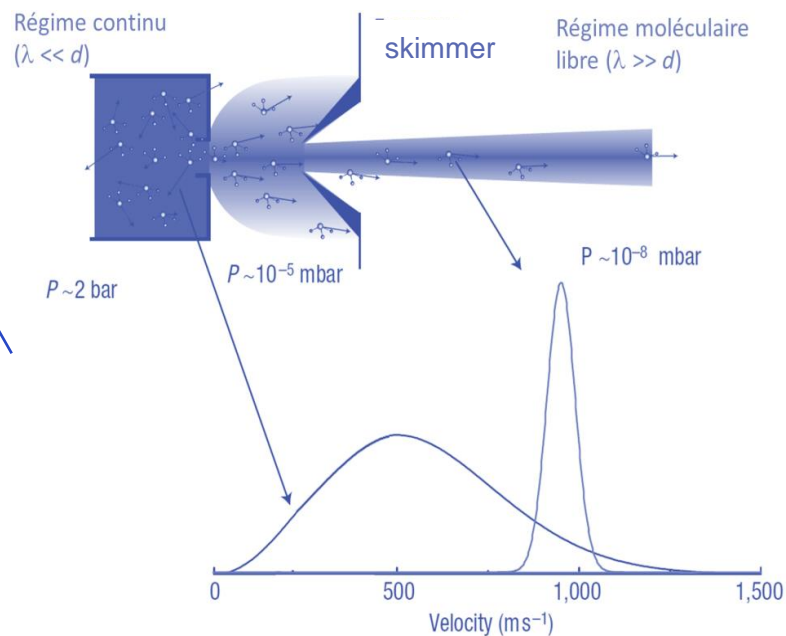
Some Cryogenic Ion Traps Results

- deuteration reactions CH_n^+ (n = 3-5) and $C_xH_y^+$
  - D. Gerlich et al, Planet. Space Sci. 50, 1287 (2002) ; O. Asvany et al, Astro. J. 617, 685 (2004) ; O. Asvany et al, Chem. Phys. 298, 97 (2005)

- CH_x^+ and CO_2^+ with H and H_2
  - D. Gerlich et al, Z. Phys. Chem 225, 475 (2011) ; G. Borodi et al, Int. J. Mass Spectrom. 280, 218 (2009)

- Laser induced charge transfer N_2^+ + Ar
  - S. Schlemmer et al, Int. J. Mass Spectrom. 185/186/187, 589 (1999)

- Radiative association reactions such as CH_3^+ + H_2
  - D. Gerlich, Phys. Scr. T59, 256 (1995)

- competition between ternary (He) and radiative association reactions CH_3^+ + H_2O
  - D. Gerlich et al, Phys. Scr. 73, C25 (2006)

- electron transfer and associative detachment of H^-/D^- with H
  - S. Roucka et al, J. Phys. Conf. 388, 082057 (2012) ; S. Roucka et al,, JPC Lett. 6, 4762 (2015)

- Reactive collision NH_2^- with H_2, inelastic collision OH^- + He
  - R. Otto et al, Phys. Rev. Lett. 101, 063201 (2008) ; D. Hauser et al, Nat. Phys. 11, 467 (2015).

CROSS BEAMS

o Absolute cross section

o Energy dependance

CCD – camera

photomultiplier

MCP + phosophorscreen

velocity map imaging spectrometer

8-pole rf ion trap 100 – 400 K

electron gun

ion lense

piezoelectric pulsed valve

Wiley-McLaren mass spectrometer

piezoelectric pulsed valve with plasma electrode

40 mm

Régime continu ($\lambda \ll d$)

Régime moléculaire libre ($\lambda \gg d$)

skimmer

$P \sim 2$ bar

$P \sim 10^{-5}$ mbar

$P \sim 10^{-8}$ mbar

Velocity (ms^{-1})

Nobel prize 1986: Y.T. Lee, Herschbach & Polanyi

S. Trippel et al., Phys. Rev. Lett. 97, 193003 (2006).
Otto, R., Mikosch, J., Trippel, S., Weidemüller, M. & Wester, R.
Nonstandard behavior of a negative ion reaction at very low temperatures.
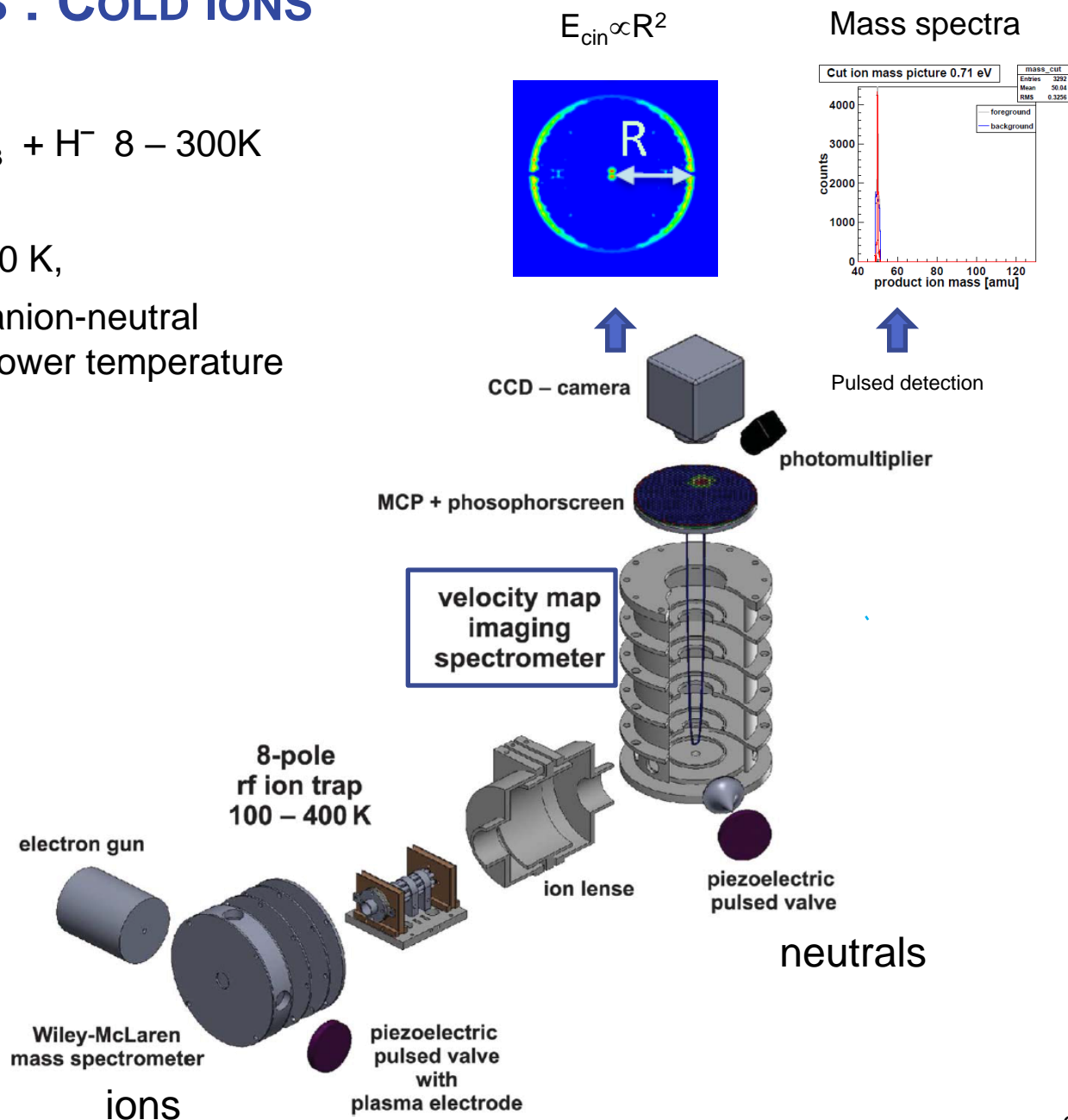*Phys. Rev. Lett. 101, 1–4 (2008).*

CROSS BEAMS : COLD IONS

○ Example :

$NH_2^- + H_2 \longrightarrow NH_3 + H^-$ 8 – 300K

Proton transfer

very inneficient at 300 K,

efficiency increase (anion-neutral complex lifetime) at lower temperature

$E_{cin} \propto R^2$

Mass spectra

CCD – camera

photomultiplier

MCP + phosophorscreen

Pulsed detection

velocity map imaging spectrometer

8-pole
rf ion trap
100 – 400 K

electron gun

ion lense

piezoelectric
pulsed valve

Wiley-McLaren
mass spectrometer

piezoelectric
pulsed valve
with
plasma electrode

ions

neutrals

- laser-cooled ions: Ca⁺ with velocity-selected CH_3F, CH_2F_2 and CH_3Cl
  - D. Gingell et al, JCP. 133,194302 (2010)

- Sympathetically-cooled ions (paramagnetic molecule): Ca⁺, OCS⁺ with ND_3 or Ca⁺, N_2H^+ with CH_3CN
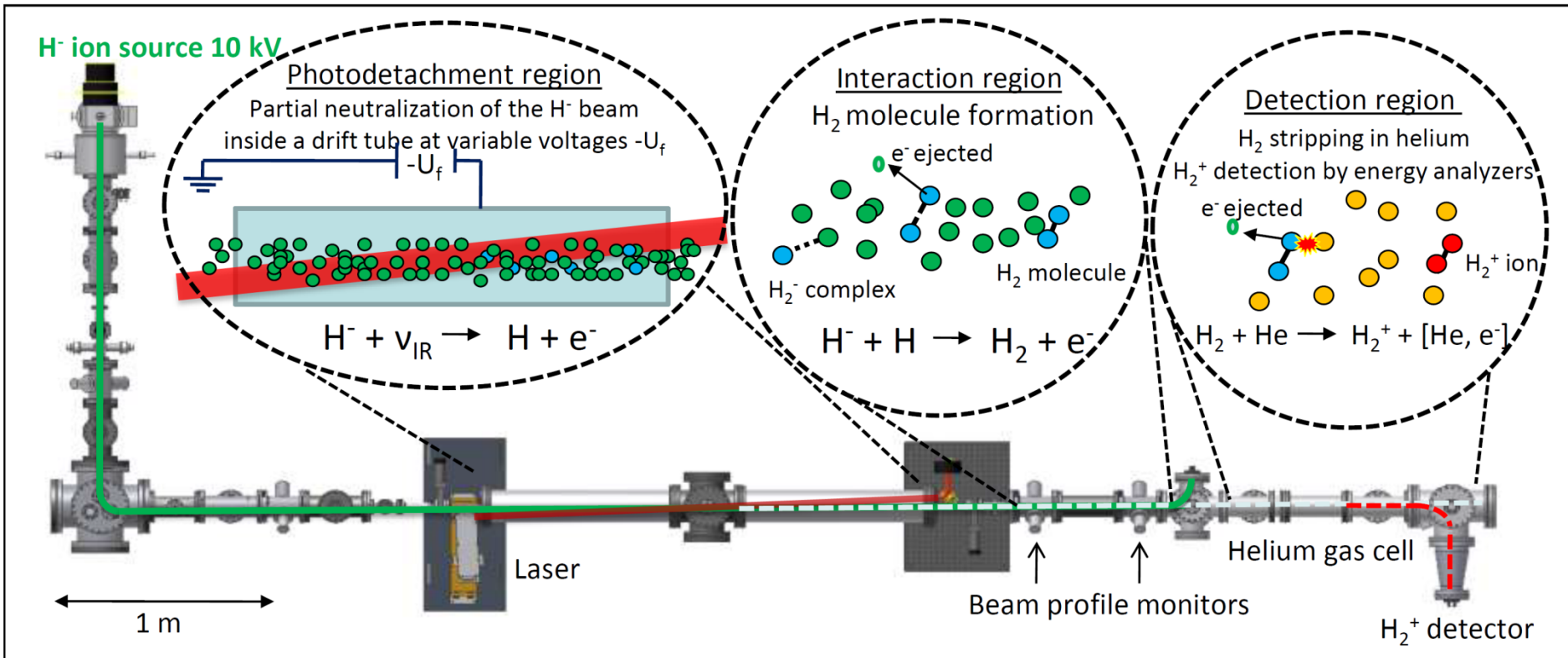
- Stark decelerator (polar molecule)

Cold Molecules: Theory, Experiment, Applications. R. Krems, B. Friedrich, W. C. Stwalley

Low-field-seeking Stark states

$$\vec{f} = -\nabla(-\vec{\mu}.\vec{\mathcal{F}})$$

38

02/09/2019
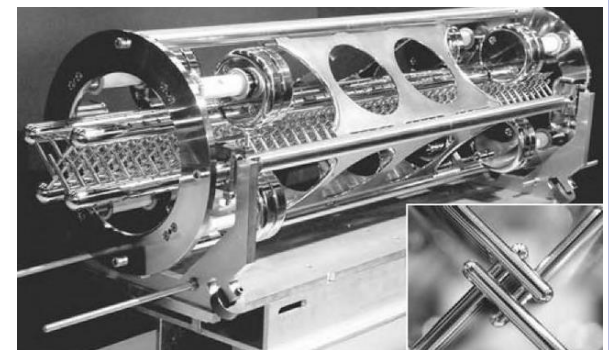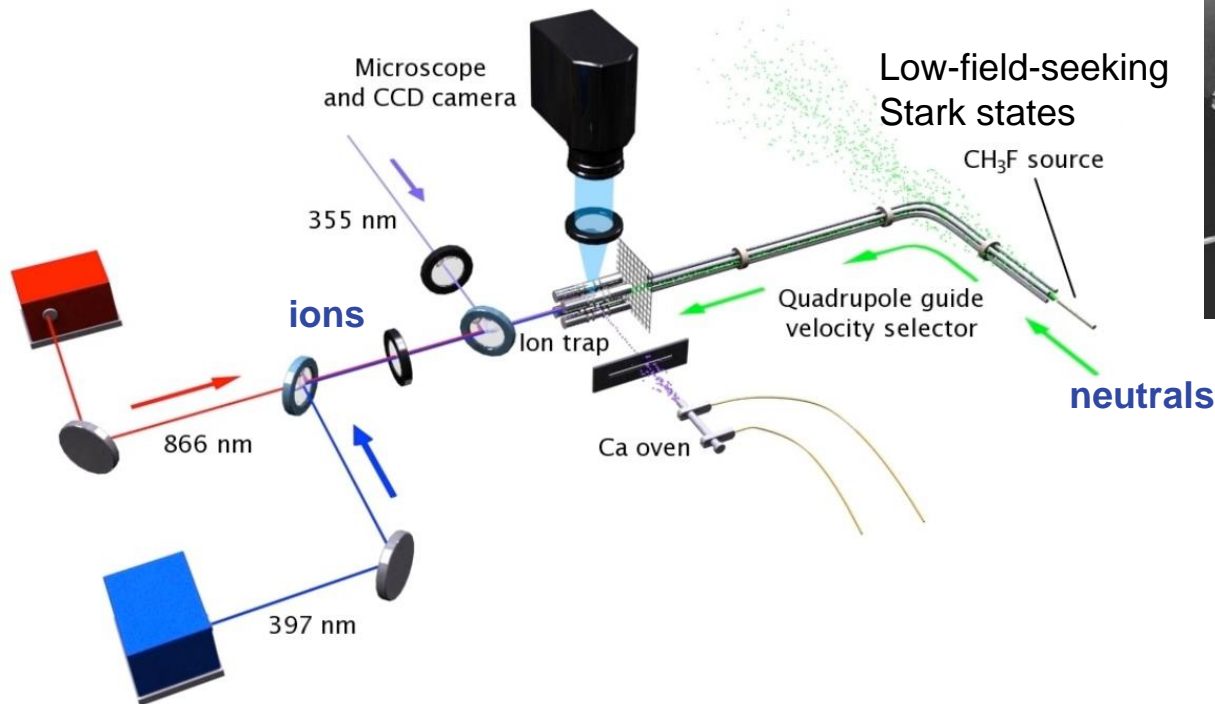
MERGED BEAMS – ASSOCIATIVE DETACHMENT : A⁻ + B → AB + e

Example: $H^- + H \longrightarrow H_2 + e$ associative detachment

Photodetachment region
Partial neutralization of the H^- beam inside a drift tube at variable voltages $-U_f$

$$H^- + \nu_{IR} \longrightarrow H + e^-$$

Interaction region
H_2 molecule formation

e⁻ ejected
H_2^- complex
H_2 molecule

$$H^- + H \longrightarrow H_2 + e^-$$

Detection region
H_2 stripping in helium
H_2^+ detection by energy analyzers
e⁻ ejected
H_2^+ ion

$$H_2 + He \longrightarrow H_2^+ + [He, e^-]$$

H^- ion source 10 kV

Laser

1 m

Beam profile monitors

Helium gas cell

H_2^+ detector

Bruhns et al, Rev. Sci. Instrum. **81**, 013112 (2010)

02/09/2019

Absolute energy-resolved measurements of the $H^- + H \rightarrow H_2 + e^-$ associative detachment reaction using a merged-beam apparatus

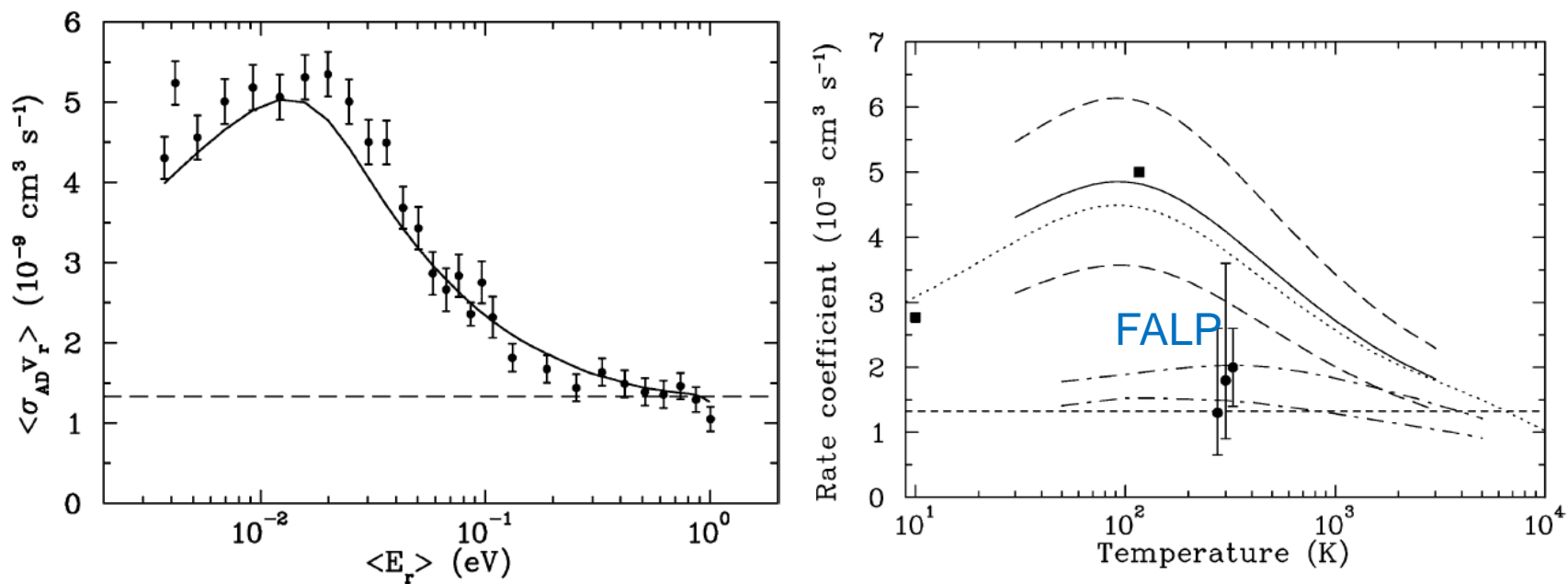H. Bruhns,[1,*] H. Kreckel,[1,†] K. A. Miller,[1] X. Urbain,[2] and D. W. Savin[1]

FIG. 8. The experimental rate coefficient $\langle \sigma_{AD} v_r \rangle$ as a function of the collision energy $\langle E_r \rangle$ is shown by the circles and the 1σ statistical uncertainty by the error bars. The solid curve gives the theoretical cross section of [9,10] times the relative velocity convolved with the experimental energy spread. The dashed curve shows the Langevin rate coefficient.

STORAGE RINGS

- ❑ DESIREE (Stokholm)
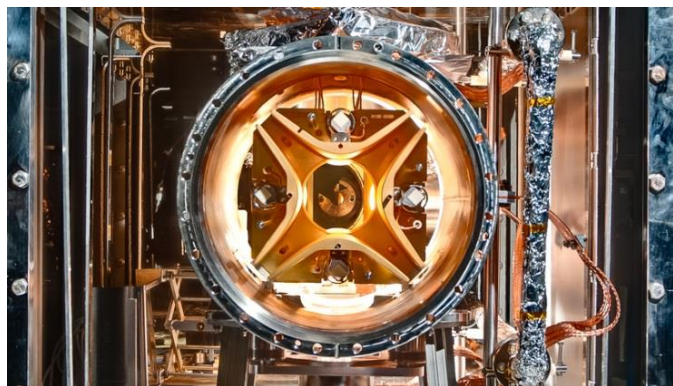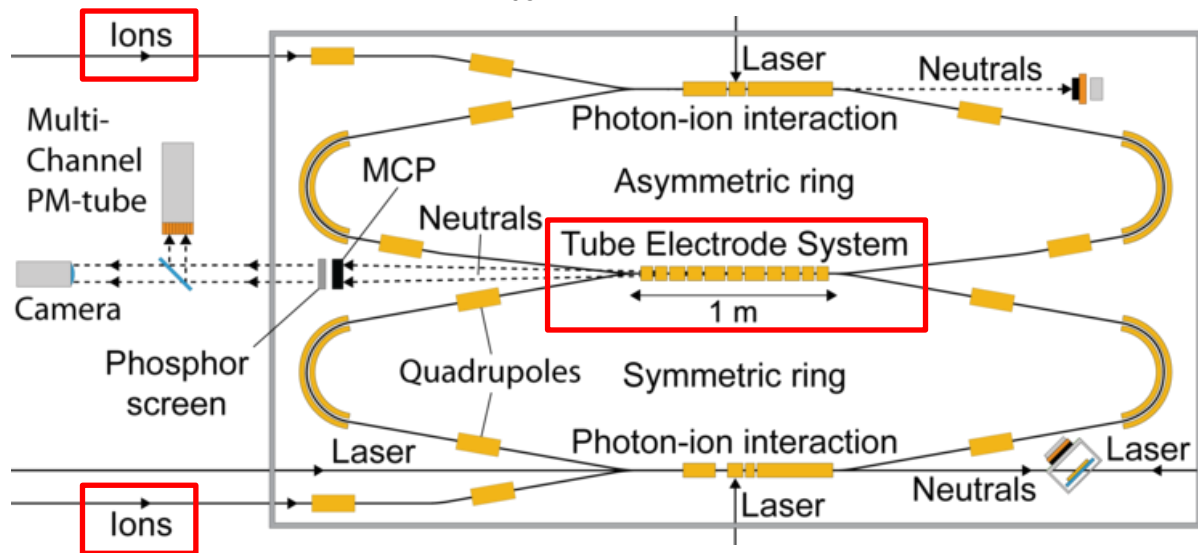 - ○ Electrostatic storage ring

$$\rho E = \frac{2E_{kin}}{q},$$

$$\rho B = \frac{1}{q}\sqrt{2mE_{kin}}.$$

P ≤ 10⁻¹³ mbar
T ≤ 13K (He)
Circumference 2x8.6 m
E_{coll} few meV

- ❑ Rotationally Cold OH− Ions : H.T.Schmidt et al, Phys. Rev. Lett. 119, 073001 (2017)
- ❑ Photodetachment thermometry on a beam of OH−, C.Meyer et al. Phys. Rev. Lett. 119, 023202 – Published 14 July 2017
- ❑ Durées de vie anneau sym. CN⁻ (N=1-4) à 10keV : H.T.Schmidt et al Rev. Sci. Instrum., 84, 5, 055115 (2013) - M. Gatchell et al 28e Intern. Conf. ICPEAC, 488, 012040 (2014)
- ❑ Operational now for anion-cation neutralization experiments. Initial reactions will concern atomic species *i.e.* C⁻ and N+

41

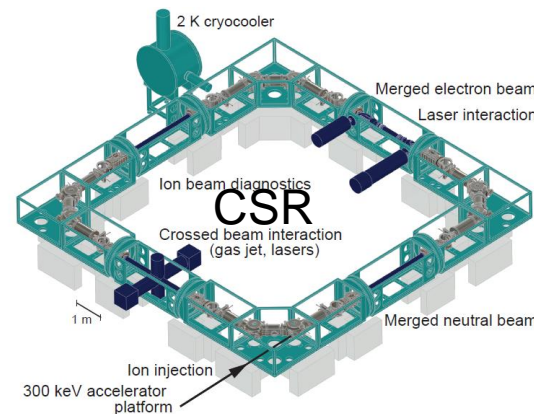# Storage Rings

- ○ ELISA (Aarhus)

- Photo excitation and laser detachment of C_{60}^- anions : Støchkel K et al, J Chem Phys. 28;139(16):164304(2013)

  - ○ CSR (Max Planck Institut)
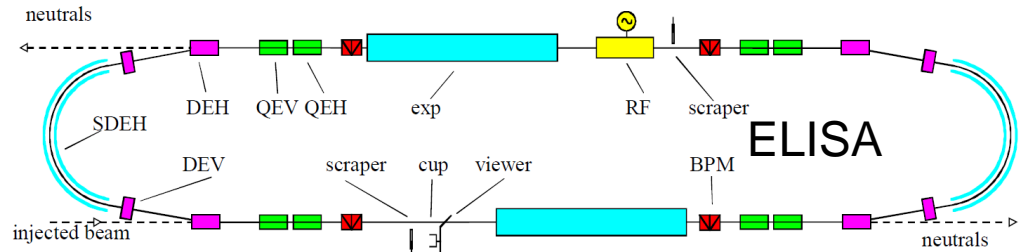
T∼225 K   P < 10^{-11} mbar
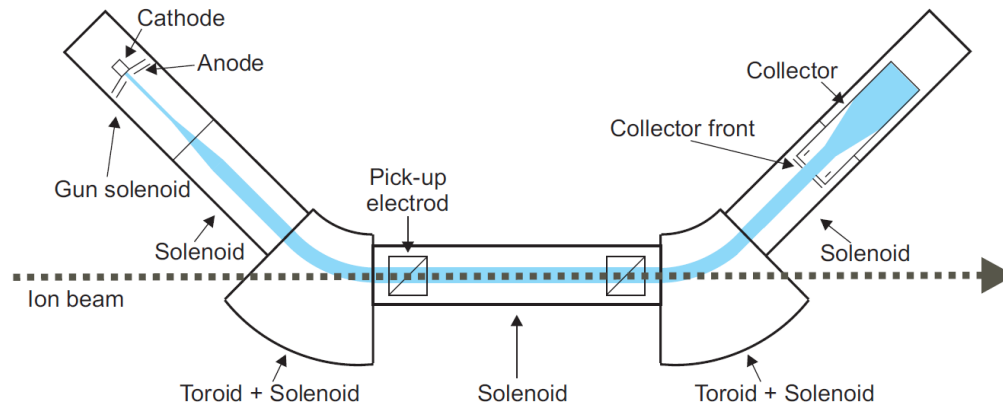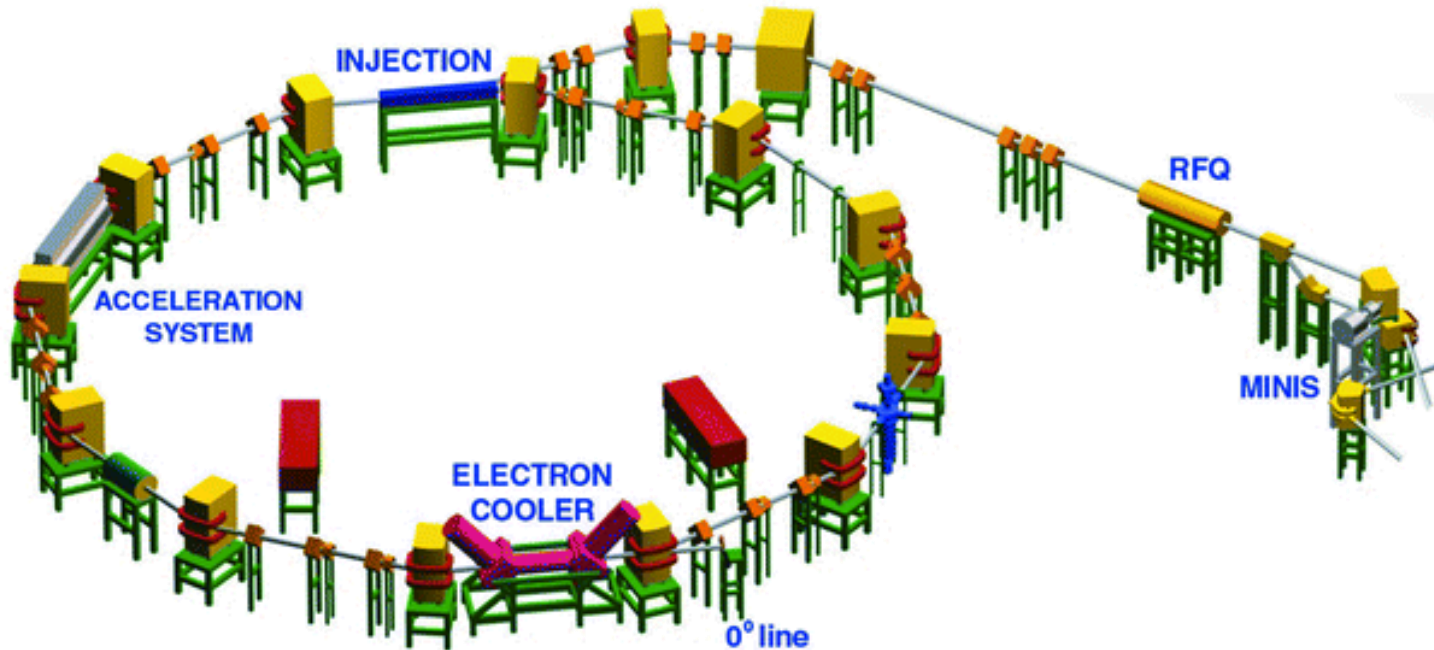Circ. 7.62 m   25 keV

T<6K
P ∼ 10^{-6} mbar
P < 10^{-13} mbar
Circ. 35m
300 keV/charge

Storage Rings - Dissociative Recombination: $AB^+ + e \rightarrow A + B$
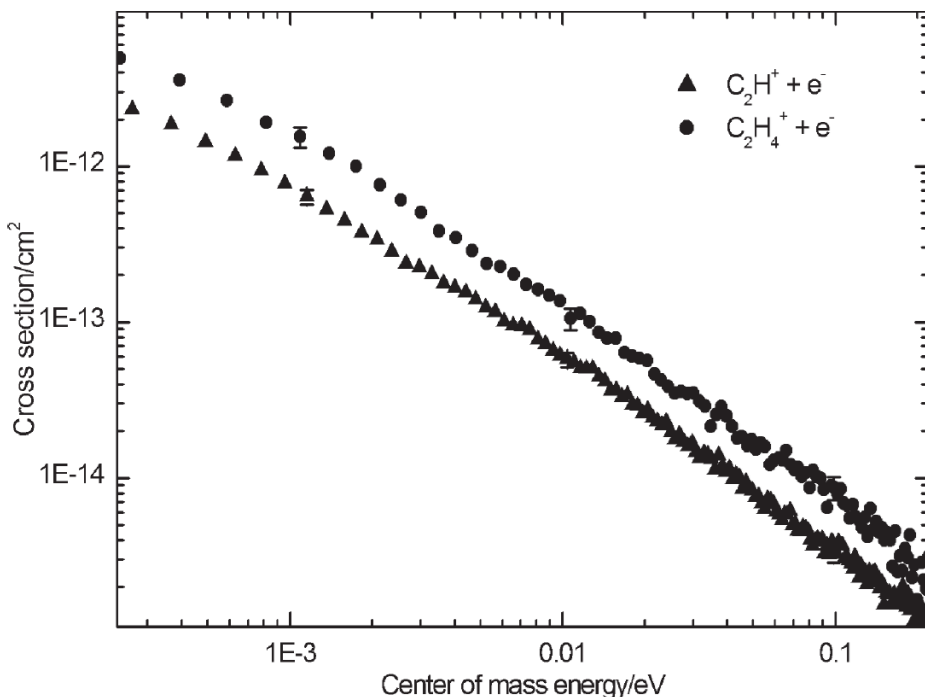
large rate coefficient

○ CRYING

02/09/2019

Dissociative recombination of C_2H^+ and $C_2H_4^+$: Absolute cross sections and product branching ratios

Anneli Ehlerding,[*a] Fredrik Hellberg,[a] Richard Thomas,[a] Shirzad Kalhori,[a] Albert A. Viggiano,[b] Susan T. Arnold,[b] Mats Larsson[a] and Magnus af Ugglas[c]


The product distribution of the dissociative recombination

C_2H^+				$C_2H_4^+$			
Products		Ratio		Products		Ratio	
$C_2 + H$	(α)	0.43 (0.03)		$C_2H_3 + H$	(α)	0.11 (0.07)	
				$C_2H_2 + H_2$	(β)	0.06 (0.03)	
				$C_2H_2 + H + H$	(γ)	0.66 (0.06)	
				$C_2H + H_2 + H$	(δ)	0.10 (0.04)	
$CH + C$	(β)	0.39 (0.04)		$CH_4 + C$	(ϵ)	0.01 (0.01)	
				$CH_3 + CH$	(ζ)	0.02 (0.02)	
				$CH_2 + CH_2$	(η)	0.04 (0.02)	
$C + C + H$	(γ)	0.18 (0.04)					

- Radiative Relaxation for ions
- High energy beam (MeV) : identification of the neutral products (except isomers)
- Used to explore the dissociative recombination
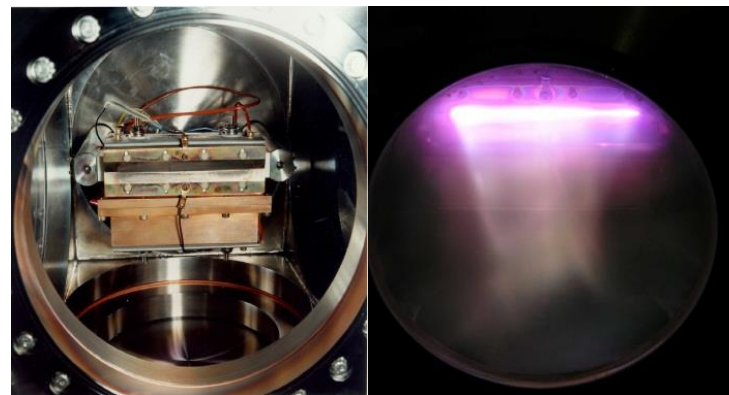- Few storage rings available to these studies

SIMULATION CHAMBER
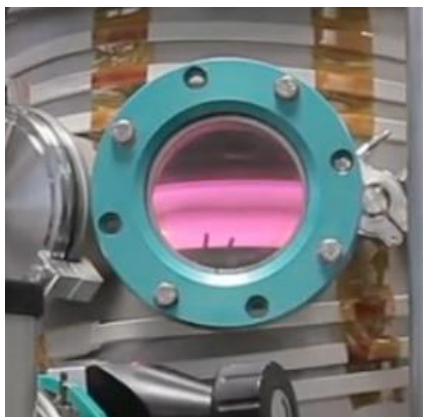
PAMPRE, LATMOS

dusty RF plasmas

- ➢ For the chemistry of Planetary Atmopsheres
- ➢ Gas mixture inside a plasma
- ➢ Products analyse (in situ or not) → chemical processes
- ➢ Option: synchrotron radiation as VUV source

Titan Haze Simulation (THS) chamber. NASA Ames COSmIC facility

THE ASTROPHYSICAL JOURNAL, 853:107 (17pp), 2018 February 1

A Model of Titan-like Chemistry to Connect Experiments and *Cassini* Observations

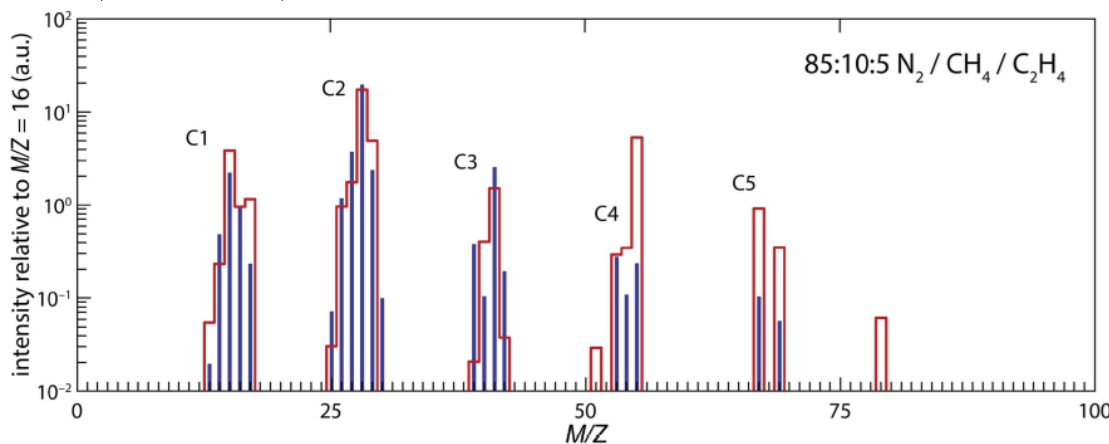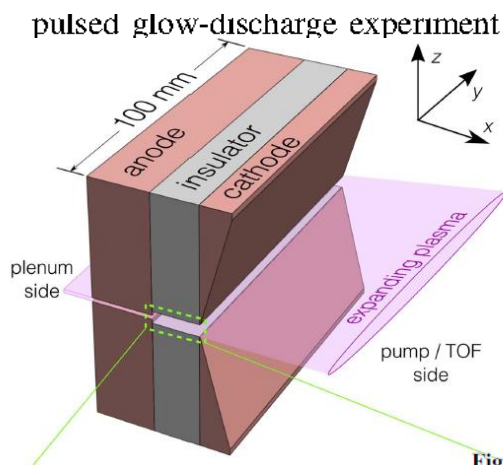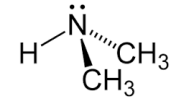Alexander W. Raymond[1], Ella Sciamma-O'Brien[2,3], Farid Salama[2], and Eric Mazur[1,4]

Figure 3. Comparison of experimental and calculated THS mass spectra for different nitrogen-based mixtures at −800 V cathode potential.

SIMULATION CHAMBER

Rapid nanoparticle nucleation by dimethylamine injection in an argon plasma

M. Mikikian[1], E. von Wahl[1], T. Lecas[1], J.-L. Le Garrec[2], J.B. Mitchell[3]

[1] GREMI, UMR7344 CNRS/Univ. Orléans, F-45067 Orléans, France, [2] IPR UMR6251 CNRS/Univ. Rennes, F-35000 Rennes, France, [3] Merl-Consulting SAS, F-35000 Rennes, France

Poster 2019

While only present as a trace in the atmosphere, dimethylamine (DMA) is considered to play an important role in the aerosol formation by stabilizing sulfuric acid-water clusters [1]. In these preliminary tests, the ability of DMA to produce nanoparticles is studied in low-pressure plasma conditions. It appears that immediately after DMA injection in an argon plasma, a huge density of nanoparticles is produced.
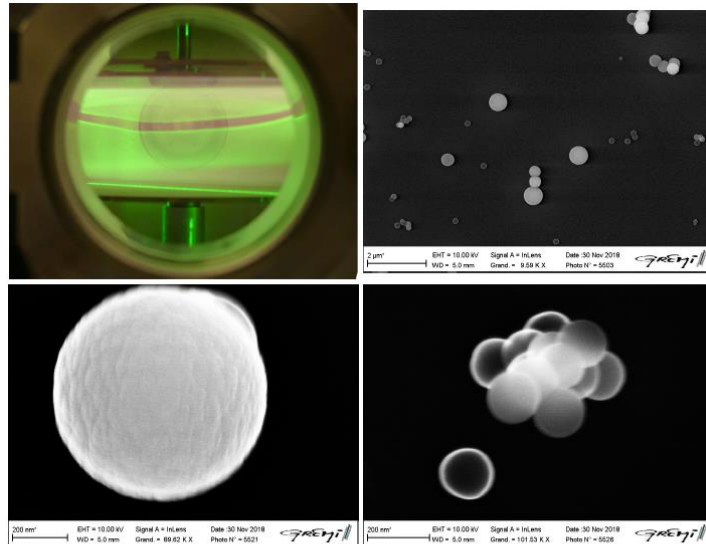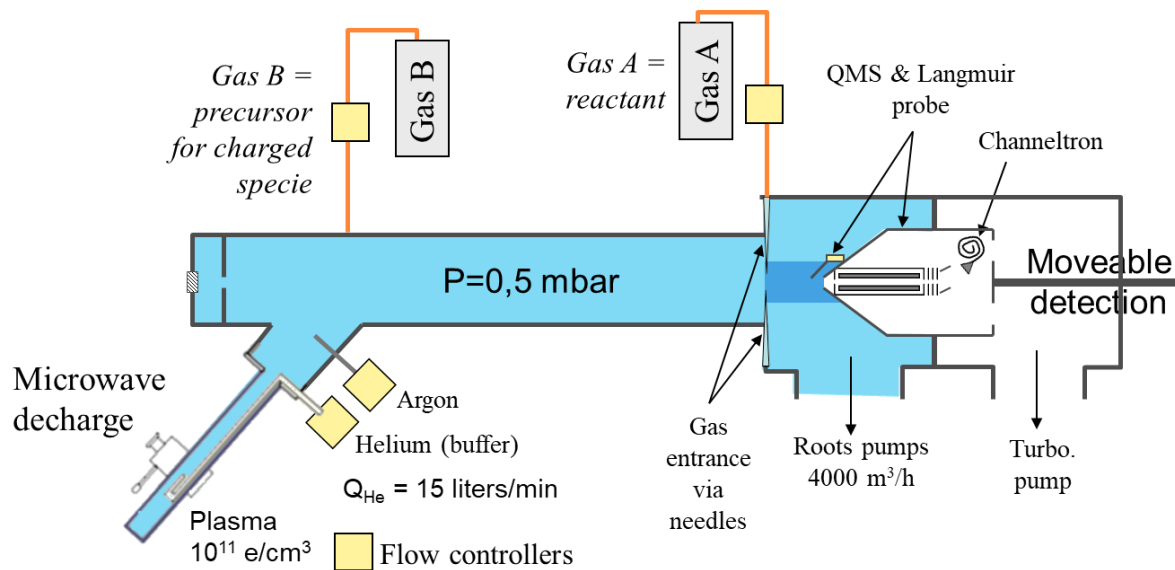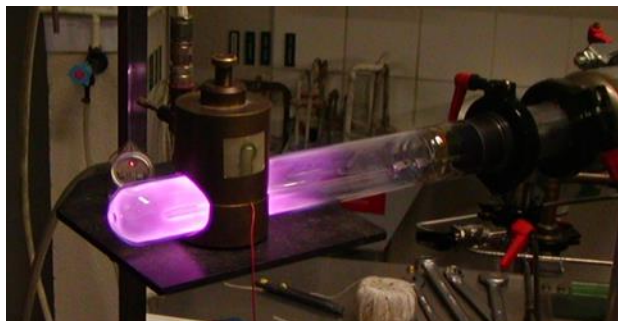

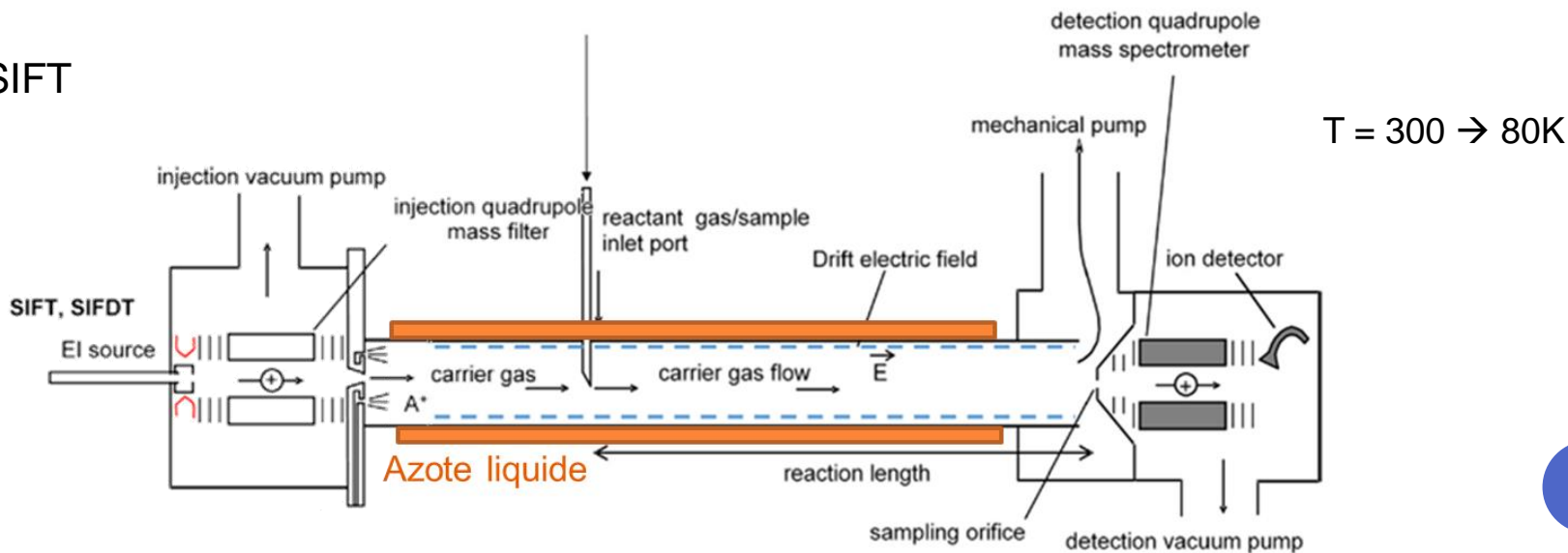**Figure:** Nanoparticle cloud grown from DMA and trapped in the plasma. SEM images of some collected nanoparticles.

[1] J. Almeida et al. Nature 502, 359 (2013)

FLOWING TUBES

- FALP-MS

Gas B =
precursor
for charged
specie

Gas B

Gas A =
reactant

Gas A

QMS & Langmuir probe

Channeltron

P=0,5 mbar

Moveable detection

Microwave decharge

Argon

Helium (buffer)

Q_{He} = 15 liters/min

Gas entrance via needles

Roots pumps 4000 m³/h

Turbo. pump

Plasma
10^{11} e/cm³

Flow controllers

- SIFT

detection quadrupole mass spectrometer

mechanical pump

T = 300 → 80K

injection vacuum pump

injection quadrupole mass filter

reactant gas/sample inlet port

Drift electric field

ion detector

SIFT, SIFDT

EI source

carrier gas

carrier gas flow

E

Azote liquide

A⁺

reaction length

sampling orifice

detection vacuum pump

Viggiano, A. A. & Paulson, J. F. J. Chem. Phys. 79, 2241–2245 (1983).

Rennes Experimental Set-up for Ion-Molecule Reactions

- **Ion-molecule reactions:** $A^{\pm} + B \longrightarrow$ products

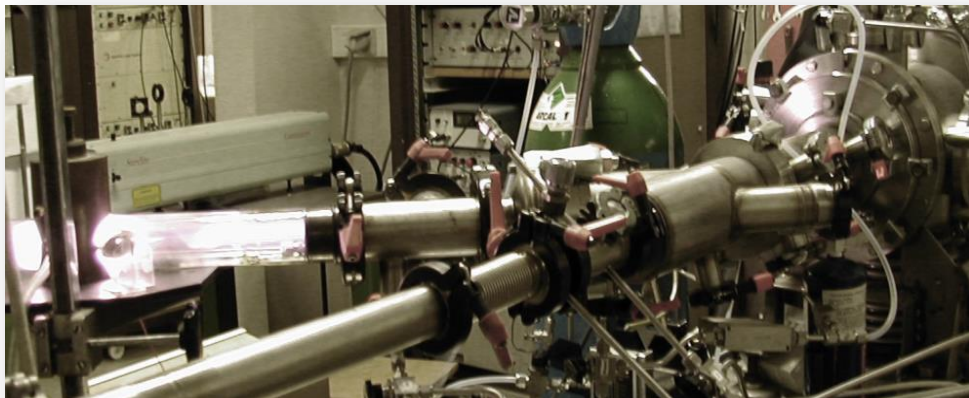 300K ————————————————————→ 12K CRESU-SIS

- **Dissociative (or not) electron attachment:** $AB + e^- \rightarrow A^- + B$; $A + e^- \longrightarrow$ products

  300K ⟶

  FALP-MS

- **Ion Recombination and Ion-neutral reaction:** $A^+ + e^-$; $A^{\pm} + B \longrightarrow$ products ;
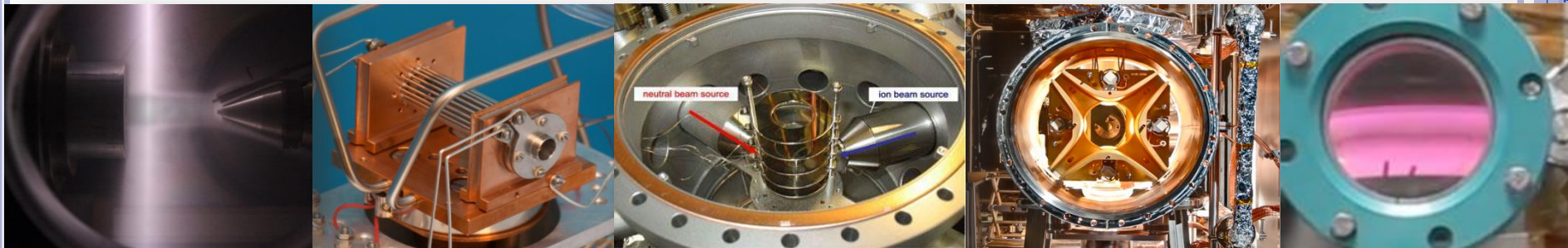
  300K ⟶

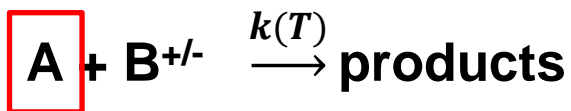 FALP-MS

FALP SET-UP 300K

CRESU-SIS SET-UP 300K → 12K

SUMMERY

Flow	Ion trap	Cross and merged Beams	Storage Rings	Simulation Chambers
$A^+ + e^- \rightarrow C + D$	$A^+ + B \rightarrow C^+ + D$	$A^+ + B \rightarrow C^+ + D$	$A^+ + e^- \rightarrow C + D$	Plasmas DC ou RF
$A^+ + B \rightarrow C^+ + D$	$A^+ + B \rightarrow AB + h\upsilon$		$A^+ + B^- \rightarrow C + D$	
$A + e^- \rightarrow A^-$				
$k(T)$	$k(T)$	$\sigma(E)$	$\sigma(E)$	Mechanisms
6—1800 K	few K	0.1 – 5 eV	> meV	T_{elec}, T_{gaz}
+ thermalisation + heavy reagent + selectivity + direct spectrosc.	+ compact + Action spectro.	+ single collision + dynamics	+ nature of neutral products	+ direct comparison to data
- Large amount of gas	- Light reagent	- Heavy experience	- Beam time	- Indirect - Complexity

49

Results with the Cresu-SIS method

CRESU-SIS METHOD

$$A + B^{+/-} \xrightarrow{k(T)} products$$

B. Joalland,[1,a] N. Jamal-Eddine,[1] D. Papanastasiou,[2] A. Lekkas,[2] S. Carles,[1] and L. Biennier[1,b]

AFFILIATIONS

[1] Université de Rennes, CNRS, IPR (Institut de Physique de Rennes)—UMR 6251, F-35000 Rennes, France
[2] Fasmatech Science and Technology SA, TESPA Lefkippos, NCSR Demokritos, 15310 Athens, Greece

[a] Current address: Department of Chemistry, Wayne State University, Detroit, Michigan 48202, USA.

Roots pumps
24000 m³/h

$P_1 = 0.1 - 3$ mbar
$T_1 = 13 - 300$K
$[n_{tot}] = 10^{16}$ cm^{-3}
$V = 3 - 17. 10^4$ cm/s

$$\frac{T_0}{T_1} = 1 + \frac{\gamma - 1}{2}M^2$$
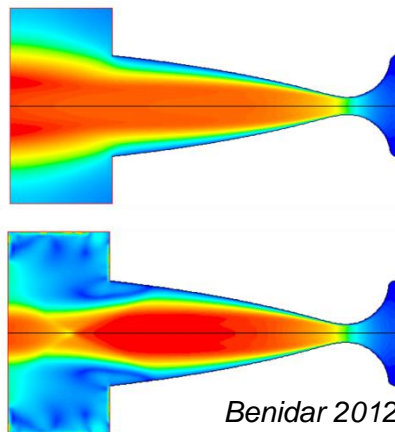
Isentropic expansion

Laval nozzle

Jet Supersonique uniforme froid

Reservoir
$P_0 = 1\text{-}100$ mbar
$T_0 = 300$K

A   He

$Q_{He} = 30 - 100$ liters/min

24 000 m³/h

Benidar 2012

02/09/2019

CRESU-SIS Method

$$A + \boxed{B^{+/-}} \xrightarrow{k(T)} \textbf{products}$$

Gas entrance:
He, Ar, B

Discharge : plasma (ions)

$P_0 \sim$ 1-10 mbar

Ion guides: Funnel + Octopole I

$P_1 \sim 10^{-2}$-10^{-3} $\longrightarrow$ Turbo. pump

Quadrupole + SEM: mass spectra /mass filter $\rightarrow$ **B** $^{+/-}$

$P_2 \sim 10^{-5}$ $\longrightarrow$ Turbo. pump

Ion guides: Octopole II + Quadrupole

$P_3 \sim 10^{-2}$-10^{-3} $\longrightarrow$ Turbo. pump

X,Y deflectors

CRESU-SIS Method

$$A + B^{+/-} \xrightarrow{k(T)} \text{products}$$

Channeltron

Quadrupole

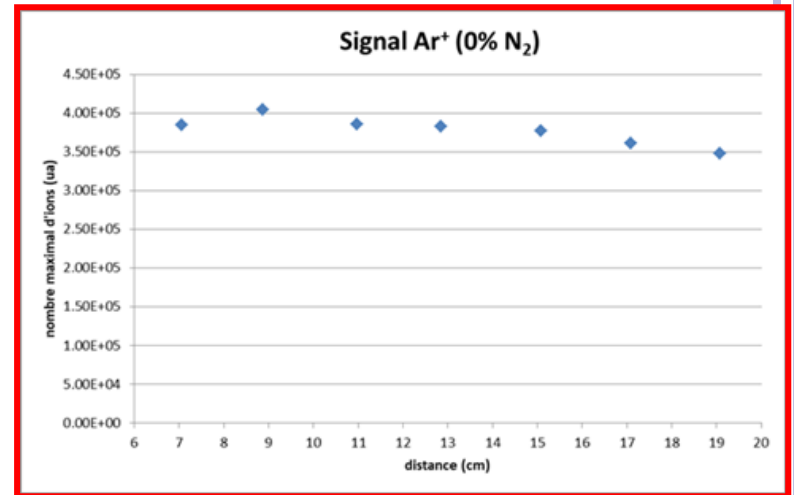Hexapole

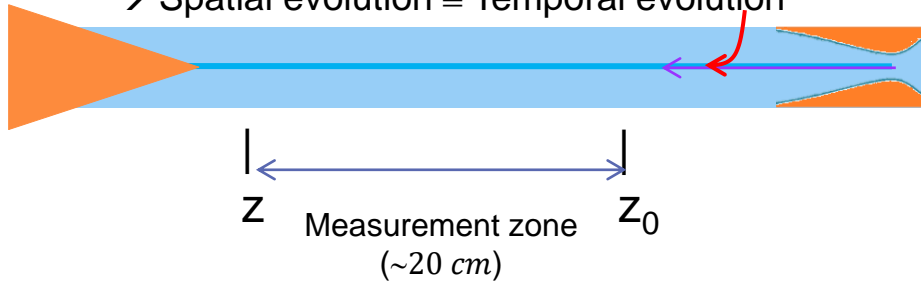Skimmer

z

z_0

Measurement zone
($\sim 20\ cm$)

Turbo.
pump

$$\frac{d[ion]}{dt}$$

- Mass spectra
- k(T) et BT(T)

CRESU-SIS: ANALYSE

$$A + B^{+/-} \xrightarrow{k(T)} \text{products}$$
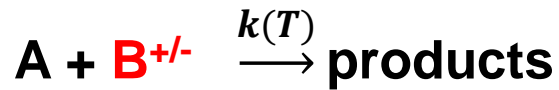
➤ Uniform beam: density, speed v, T
→ Spatial evolution ≡ Temporal evolution

z   Measurement zone z_0
         (~20 cm)

Pseudo 1st order [A]>>[B $^{+/-}$] : $\dfrac{d[B^{+/-}]}{dt} = -k[B^{+/-}][A] \Leftrightarrow \ln\left(\dfrac{[B^{+/-}]_z}{[B^{+/-}]_{z0}}\right) = -[A]k\dfrac{1}{v}(z - z_0)$

Signal Ar⁺ (0% N₂)

Ar$^+$ + N$_2$ @ 36K
[N$_2$]=4.5E14 cm^{-3}

Ar$^+$ + N$_2$ @ 36K
k = -3.07E-11 cm^3/s

CRESU-SIS: First Results

$$Ar^+ + N_2 \xrightarrow{k(49K)} N_2^+ (v=0) + Ar \quad \text{exoergique 0.18 eV ; dominant} < 140K$$
$$\longrightarrow \quad N_2^+ (v=1) + Ar \quad \text{endoergique 0.09 eV ; dominant aux hautes T°,}$$
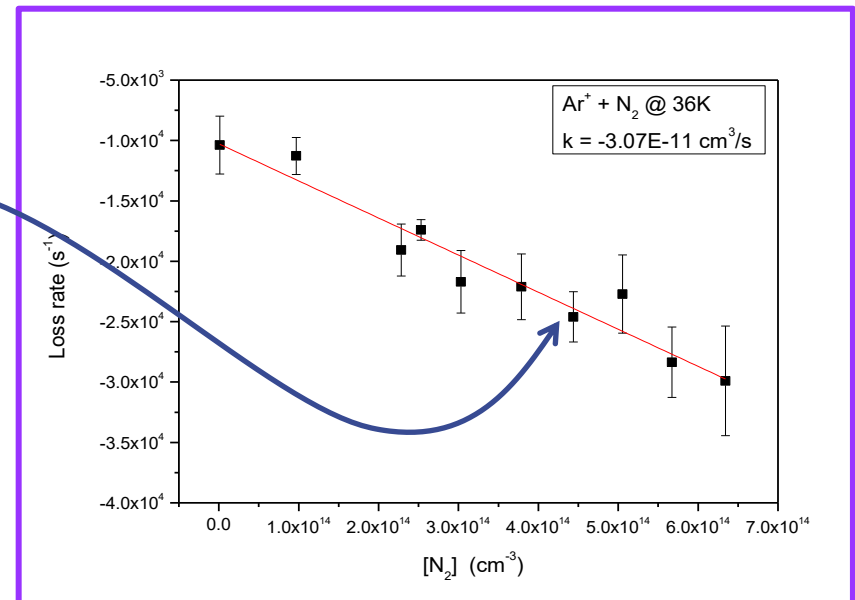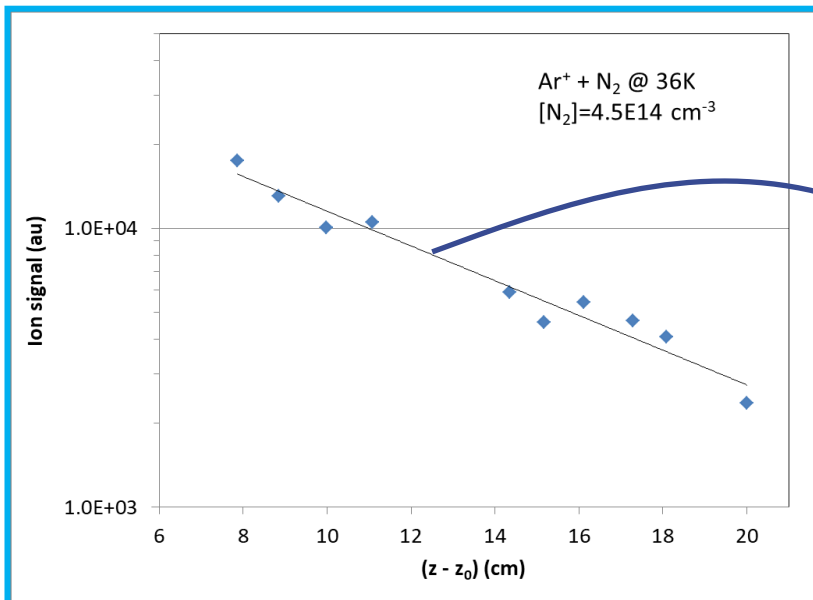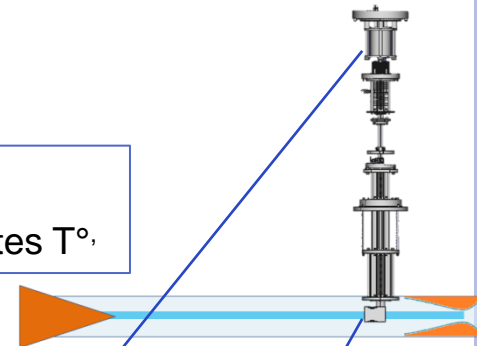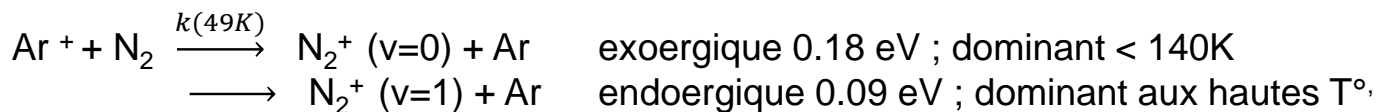
$Ar^+ (^2P_{1/2}) \xrightarrow{He} Ar^+ (^2P_{3/2})$: 4.10^{-11} cm^3/s [a]
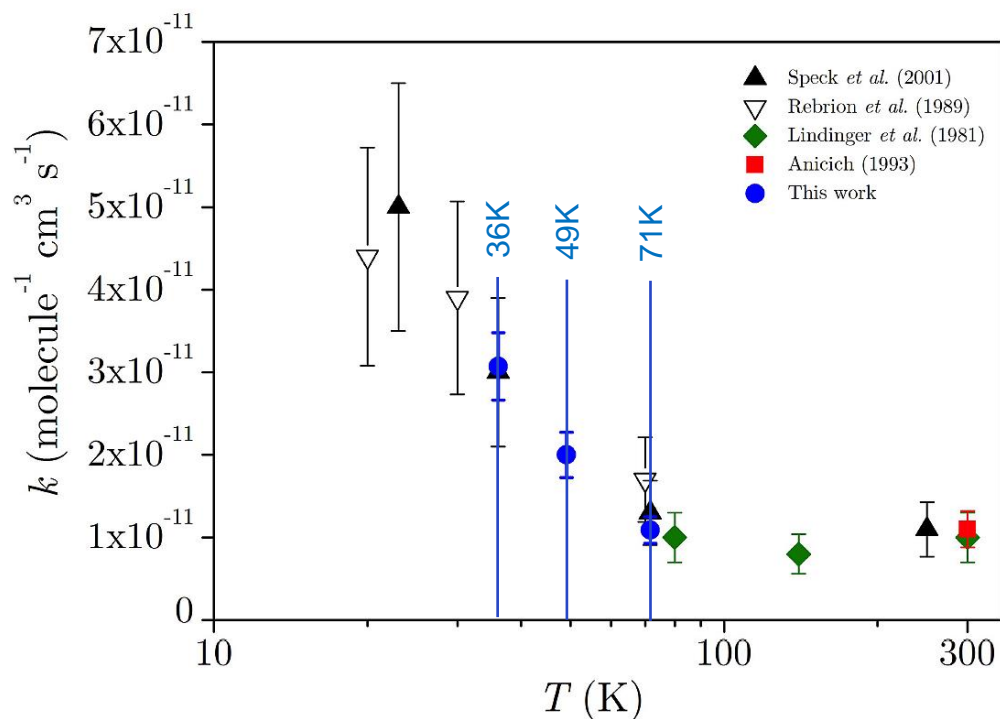SIS : [He] ~ 5.10^{16} molecules/cm^3 → Relaxation of the spin-orbital states: $\tau_{relax} < 1\mu s \Rightarrow$ directly in the plasma source

CRESU jet: [He] > 5.10^{16} molecules/cm^3
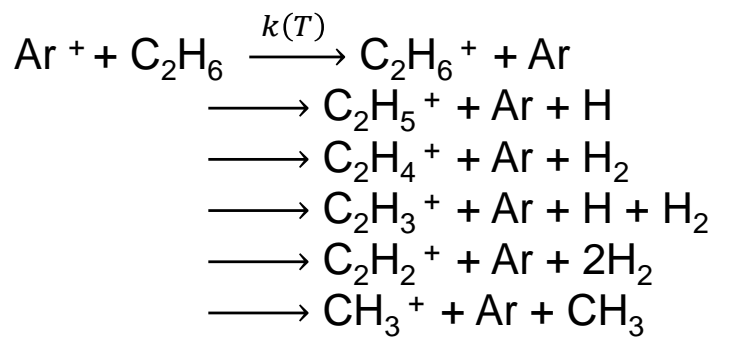→ Time between 2 collisions: qq 10^{-10} s $\Rightarrow$ Translational and rotational relaxations are effective

Rate coefficient for the Ar$^+$ + N$_2$ reaction in function of temperature.
▲▽ ● Old and new CRESU measurements ; ◆ SIFT measurements
■ average room temperature value (Anicich 2003)

	T (K)	This work	Previous measurements	Langevin	[n]
			$k (10^n$ molecule^{-1} cm^3 s^{-1})		
Ar$^+$ + N$_2$	36[a]	3.07 ± 0.27	3.00[b]	75.5	[−11]
	49[a]	2.00 ± 0.19	...		
	72[a]	1.09 ± 0.12	1.30[b]		

a= estimated temperatures (±1K) with impact pressure and LIF measurements; b= CRESU measurements with a pulsed injection of ions

55

02/09/2019

CRESU-SIS: First Results

$$Ar^+ + C_2H_6 \xrightarrow{k(T)} C_2H_6^+ + Ar$$
$$\longrightarrow C_2H_5^+ + Ar + H$$
$$\longrightarrow C_2H_4^+ + Ar + H_2$$
$$\longrightarrow C_2H_3^+ + Ar + H + H_2$$
$$\longrightarrow C_2H_2^+ + Ar + 2H_2$$
$$\longrightarrow CH_3^+ + Ar + CH_3$$

➢ $k(\forall\, T) \approx k_L = 1{,}16.10^{-9}$ cm^3/s
➢ k(T) and RB(T) are independant of the Temperature

Ar$^+$ + C$_2$H$_6$

T = 36.1 K

Loss rate (s^{-1}) vs [C$_2$H$_6$] / cm^{-3}

	T (K)	This work	Previous measurements	Langevin	[n]
			$k\ (10^n$ molecule^{-1} cm^3 s$^{-1})$		
Ar$^+$ + C$_2$H$_6$	36[a]	1.20 ± 0.12	0.86[b]	1.16	[−9]
	49[a]	1.33 ± 0.13	. . .		
	300	. . .	0.92[c]		
	380	. . .	1.14[d]		

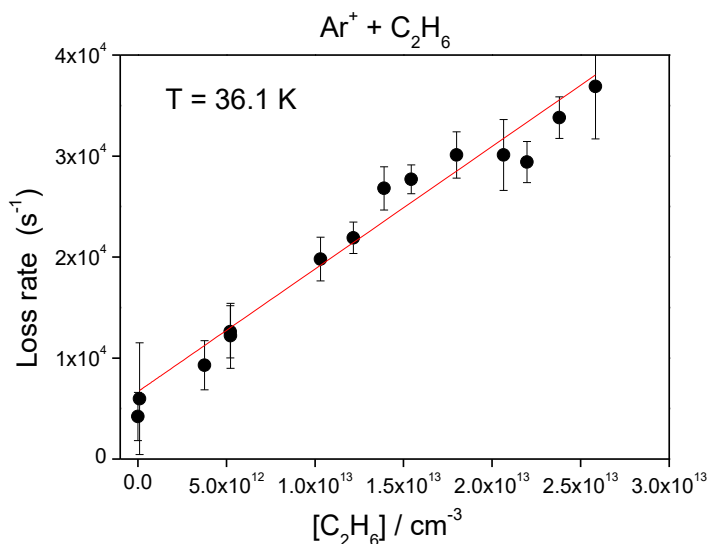a= estimated temperatures (±1K) with impact pressure and LIF measurements; b= CRESU measurements with a pulsed injection of ions ; c= FA (Flowing Afterglow) measurements ; d = SIFT (Selected Ion Drift Tube) measurements
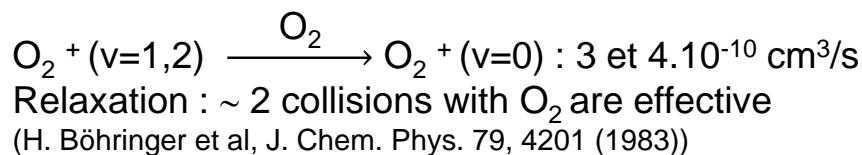
Products	T (K) =	Branching ratios		
		This work[a]	Previous measurements	
Ar$^+$ + C$_2$H$_6$ →		49	300[b]	380[c]
C$_2$H$_6^+$ + Ar		0.03	. . .	. . .
C$_2$H$_5^+$ + H + Ar		0.10	0.08	0.18
C$_2$H$_4^+$ + H$_2$ + Ar		0.23	0.22	0.18
C$_2$H$_3^+$ + H$_2$ + H + Ar		0.36	0.42	0.38
C$_2$H$_2^+$ + 2H$_2$ + Ar		0.23	0.23	0.20
CH$_3^+$ + CH$_3$ + Ar		0.05	0.05	0.06

a= error bars: systematic contributions (±0.02) and statistical contributions (±5%) ; b= FA measurements ; c = SIFT measurements
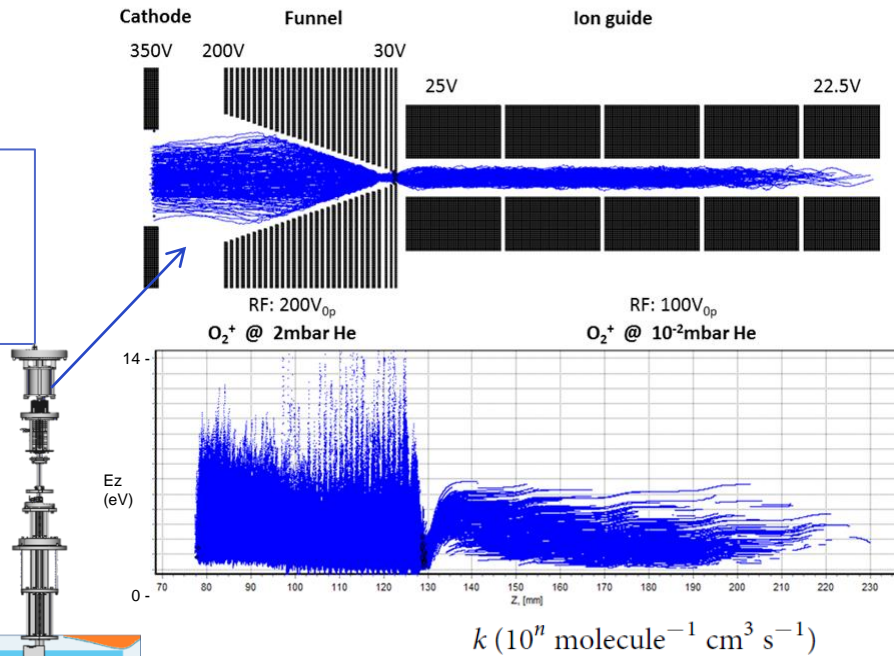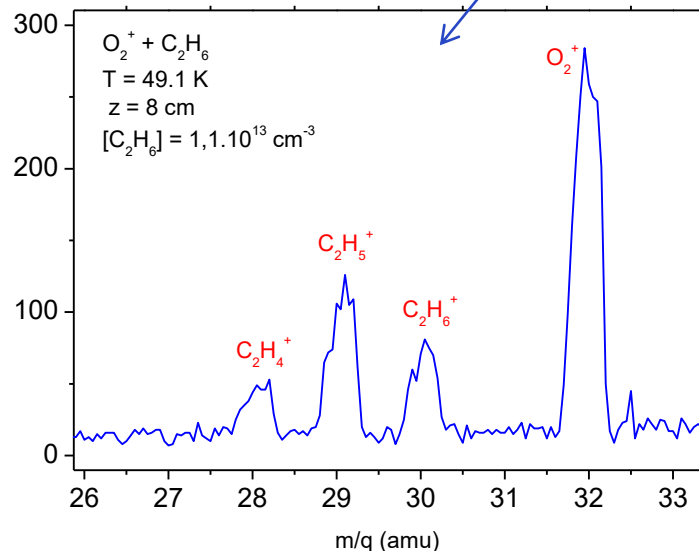
02/09/2019

CRESU-SIS: First Results

$$O_2^+ + C_2H_6 \xrightarrow{k(49K)} C_2H_6^+ + O_2 \qquad 30\%$$
$$\longrightarrow C_2H_5^+ + O_2 + H \qquad 55\%$$
$$\longrightarrow C_2H_4^+ + O_2 + H_2 \qquad 15\%$$

$$k(\forall T) \approx k_L = 1{,}22.10^{-9}\ cm^3/s$$

$$O_2^+ (v=1,2) \xrightarrow{O_2} O_2^+ (v=0) : 3\ et\ 4.10^{-10}\ cm^3/s$$

Relaxation : ~ 2 collisions with O_2 are effective
(H. Böhringer et al, J. Chem. Phys. 79, 4201 (1983))
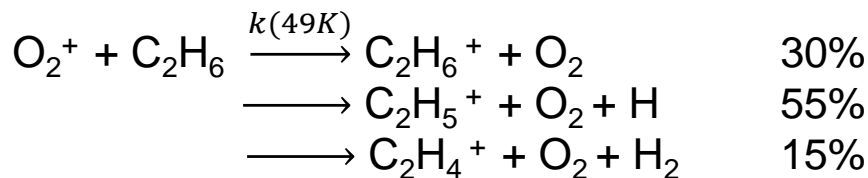
$[O_2] > 5.10^{14}$ molecules/cm^3
Simulations (1% O_2) : ~8 collisions
between cathode / funnel end

$O_2^+ + C_2H_6$
T = 49.1 K
z = 8 cm
$[C_2H_6] = 1{,}1.10^{13}\ cm^{-3}$

$C_2H_4^+$ $C_2H_5^+$ $C_2H_6^+$ O_2^+

ion signal (au) vs m/q (amu)

	T (K)	This work	Previous measurements	Langevin	[n]
$O_2^+ + C_2H_6$	49[a]	1.21 ± 0.13	...	1.22	[-9]
	300	...	$1.21^{[e]}/1.1^{[f]}$		

$k\ (10^n\ molecule^{-1}\ cm^3\ s^{-1})$

Branching ratios

Products	T (K) =	This work[a] 49	Previous measurements 300[d]
$C_2H_6^+ + O_2$		0.26	0.30
$C_2H_5^+ + O_2 + H$		0.57	0.55
$C_2H_4^+ + O_2 + H_2$		0.17	0.15

a= estimated temperatures (±1K) with impact pressure and LIF measurements; b= CRESU measurements with a pulsed injection of ions ; c= FA (Flowing Afterglow) measurements ; d,f = SIFT (Selected Ion Drift Tube) measurements ; e= Time resolved ion mass spectrometry at atmospheric pressure (238–458)K
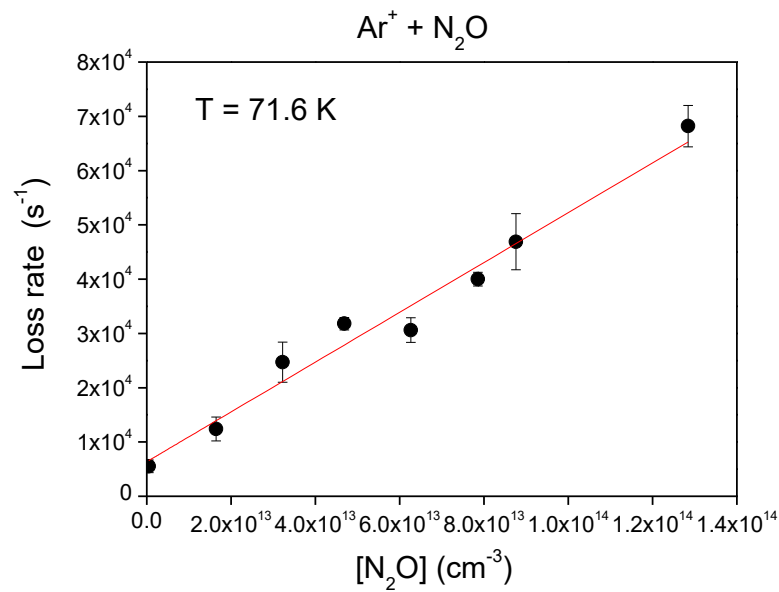
CRESU-SIS: First Results

$$Ar^+ + N_2O \xrightarrow{k(49K)} N_2O^+ + Ar \quad 100\%$$

$\mu_{N2O} = 0{,}16$ D

Uniform supersonic flow
$T = 49$ K ; $t = 95$ μs
$[N_2O] = 0.0 - 5.7 \times 10^{12}$ cm^{-3}

Ion transfer line
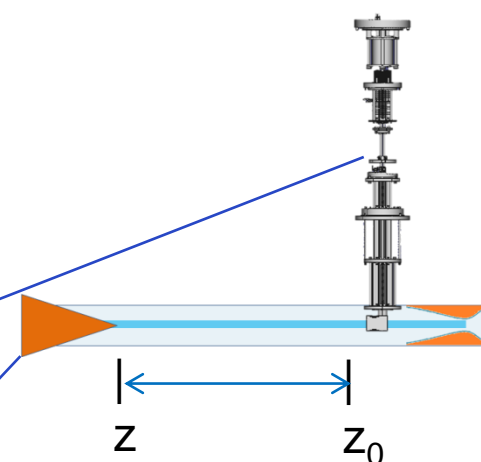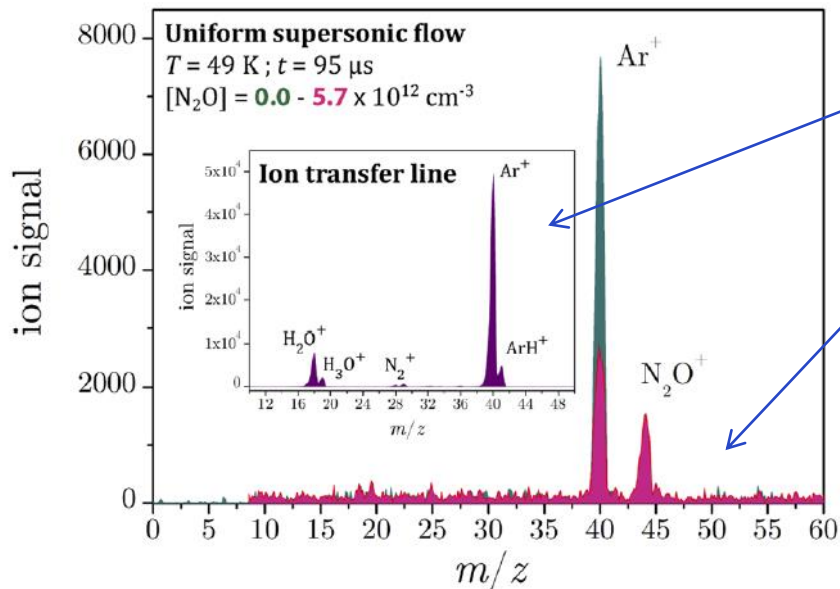
95 μs → $(z-z_0)=15$ cm ($v=15.7 \times 10^4$ cm/s)

$Ar^+ + N_2O$

T = 71.6 K

	T (K)	This work	Previous measurements	Langevin	$[n]$
$Ar^+ + N_2O$	36[a]	4.6 ± 0.5	...	8.9	$[-10]$
	49[a]	5.7 ± 0.9	...		
	72[a]	4.8 ± 0.6	...		
	300	...	$3.3^g/3.0^h$		

k (10^n molecule^{-1} cm^3 s^{-1})

02/09/2019

- Negative ion reactivity:
- Cinétiques des réactions $C_xH_y^-$ + HC_3N, X $\longrightarrow$
- Cinétiques des réactions $C_{x>3}N^-$ + HC_3N, X $\longrightarrow$
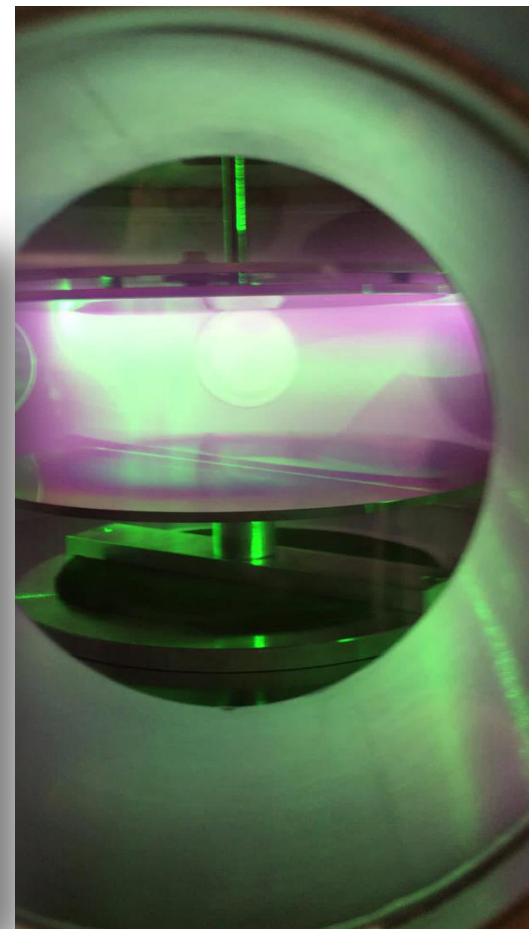
THANKS !!

Jean-Claude Guillemin

Yann Trolez

Emmanuel Raptakis

Dimitris Papanastasiou

Baptiste Joalland

Nour Jamal Eddine